Physical Metallurgy and Drawability of Extra Deep Drawing and Interstitial Free Steels

Kumkum Banerjee

Research and Development Department, Tata Steel Ltd., Jamshedpur,
India

1. Introduction

The aim of this review is to present the underlying physical metallurgy for the development of aluminium killed (Extra deep drawing--EDD) and interstitial free (IF) steels, their recrystallization texture and its subsequent impact on the formability of these steels. A plethora of literature is available and a number of review articles have appeared previously (**Hutchinson, 1984; Ray et al, 1994**). These contributions dealt broadly with the development of cold rolled and annealed textures till 1994 and since then further advances in research had been made on the subject and the present article is intended to provide the progresses made on the subject till date, while also giving a critical review of the subject as a whole.

The automotive industry aims to reduce the weight of outer-body car panels while maintaining strength, formability and dent resistance. However, conventional high strength sheet steels have insufficient formability to meet the drawing requirements of today's more complex outer-body car panels. In the recent years low and ultra low carbon steels like extra deep drawing aluminum killed, interstitial free, interstitial free high strength and bake hardening steels are known for their formability and are extensively used for the auto bodies.

Texture is an important parameter of steel sheets as it induces plastic anisotropy that can be beneficial to drawability of steels (**Hosford & Backholen, 1966; Lankford et al., 1950; Yoshicla, 1974**). The anisotropy is conveniently measured in terms of r_m-value that is the ratio of true width strain to true thickness strain determined through standard tensile tests. r_m-value varies essentially with respect to rolling direction of the sample. Thus, an average of the r-values is taken as r_m, which is expressed through the expression--$(r_0 + 2r_{45} + r_{90})/4$ – termed as 'normal anisotropy'--where the subscripts, 0, 45 and 90 refer to the tensile specimens with parallel to, 45° and 90° to the rolling direction of the steel sheet. Isotropic steels have r_m-value around 1 while steels suitable for deep drawing applications should have r_m-value 1.8 (Holie, 2000).

High r_m-values correlate well with good deep drawability (**Lankford et al., 1950).** Good drawability also diminishes the edge splitting tendency during hole- expansion tests (**Klein & Hitchler, 1973**). The favourable texture for good deep drawability is a large fraction of the grains oriented with {111} planes parallel to the plane of a sheet (**Whiteley & Wise, 1962**). To ensure satisfactory drawability in these steels, i. e. to increase the depth

of drawing and avoid the crack during deep drawing process and at the same time to make the edge on the top of a drawn cup smooth without the phenomenon of earing, the deep drawing sheet is required to possess high plastic anisotropy, r_m and low normal anisotropy, Δr. In other words, to maximize r_m-value and minimize Δr-value, {111}<112> and {111}<110> components of γ-fiber **(Figure 1)** (**Kestens et al., 1996**) are the ideal crystallographic textures for deep drawing steel, because the correct texture gives the proper orientation of slip system so that the strength in the thickness direction is greater than that in the plane of the sheet. If {100} plane parallels rolling plane, the strength is lowest in the thickness direction of sheet. This, in turn, adversely influences the formability of the sheet. The {111}/{l00} intensity ratio is reported to be linearly related to r_m (**Held, 1965**) and can easily be determined using X-ray diffractometer measurements of the (222) and (200) lines.
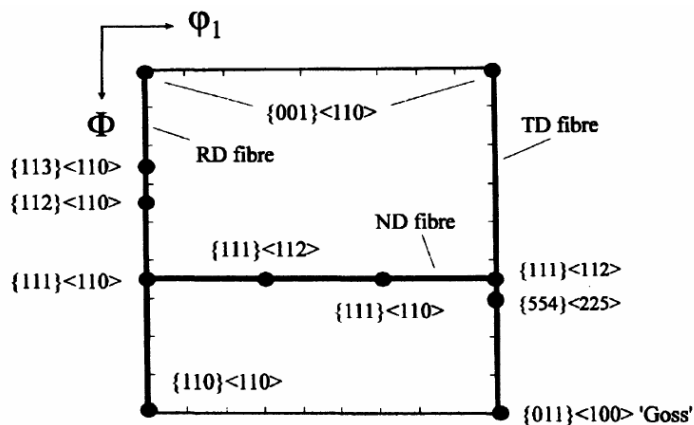

Fig. 1. $\varphi2=45°$ section of Euler space showing the ideal bcc rolling and recrystallization texture components (**Kestens et. al., 1996**)

2. Recrystallization texture

In several cases, after only small cold deformation, nearly random textures are produced. However, on annealing after very heavy cold reductions, a strong recrystallization texture is usually obtained that may involve the partial retention of the deformation texture but quite often a very different but very strong new texture forms. Thus, the changes in texture that occur during the recrystallization process can be massive while compared to previous texture of the deformed state and in some cases, replaced by an entirely different texture (**Doherty et al., 1997**).

Two major theories exist for the formation of recrystallization texture-- described as 'oriented nucleation' and 'oriented growth' (**Doherty et al., 1988 & Samajdar, 1994**). Oriented nucleation is the hypothesis that explains, grains with an orientation that dominates the fully recrystallized texture, nucleate more frequently than do grains of all other orientations. In other words, the oriented nucleation theory assumes orientation selection in the nucleation process based on the orientation dependence of the deformation energy stored in the grains during cold rolling (Tsunoyama, 1998). The high

stored energy in (111) grains is considered to be responsible for the (111) orientation nucleation and growth. However, the energy stored in (110) grains is higher than that in (111) grains and another mechanism is required for the preferential development of (111) orientation. To describe the orientation nucleation theory quantitatively, for example for the most discussed case of the formation of 'cube' texture after the recrystallization of heavily rolled FCC metals such as Cu or Al, the fraction of grains, by number, within a selected misorientation, of 10 or 15° from exact cube, α_c, must be normalized by the fraction expected in a random grain structure, α_r (Doherty, 1985). The condition for a strong 'oriented nucleation' effect is that: $\alpha=\alpha_c / \alpha_r$. That is, the frequency of the formation of the new cube grains is much higher than the expected random frequency, so many of the grains will have the special orientation.

While, the oriented growth theory is based on the orientation dependence of the grain boundary mobility **(Tsunoyama, 1998).** In this theory, orientation relations between recrystallization nuclei and the deformed matrix is responsible for the texture development. However, no significant experimental evidence of oriented growth has been obtained for IF steels until now, even with modern techniques like EBSD (Electron Back-Scattered Diffraction). The oriented growth factor, β, is determined by the relative sizes $\overline{d_c} / \overline{d_r}$ of the cube to the average grains (**Doherty, 1985**). That is, there is a strong oriented growth effect if: $\beta= \overline{d_c} / \overline{d_r} >> 1$ (**Martin, et al., 1997**).In the opinion of Doherty et al (**Doherty et al., 1997**), the two theories of oriented nucleation and oriented growth should be renamed as: (i) the grain frequency effect; and (ii) the grain size effect, respectively. The reason behind the change was i) the nucleation involves only the growth of a particular subgrain and the terms, oriented nucleation and oriented growth are often taken to indicate specific mechanisms for the frequency or size advantage. Thus, the usage of "frequency" and "size effect" helps avoid such confusion.

The steel recrystallization texture is of major industrial importance. It is found that recrystallization in a cold-worked low carbon steel is mainly controlled by the oriented nucleation theory/grain frequency effect that is governed by the orientational dependence of the stored deformation energy (**Hölscher et al, 1991.**) The two key recrystallization texture components in steel are $\{110\}<1\,\overline{1}\,0>$ and $\{554\}<22\,\overline{5}>$. The latter component is just a few degrees away from another recrystallization texture component $\{111\}<112>$ (**Hatherly & Hutchinson, 1979**). During recrystallization two major changes take place. The orientation $\{001\}<110>$ and the orientation spread surrounding the partial α-fiber texture gets eliminated after annealing and some redistribution of intensity in the fiber texture with $\{111\}$ planes parallel to sheet.

The strength of $\{111\}$ texture determines the drawability of low carbon and extra low carbon steels. The strength of $\{111\}$ texture in turn is influenced by chemistry of the steel (**Perera et al., 1991; Wilshynsky-Dresler et al., 1995**) and the prior technological processing steps, such as hot rolling (Wilshynsky-Dresler et al., 1995 & Perera et al., 1991), cold rolling (**Perera et al., 1991**) and annealing (**Perera et al., 1991, Wilshynsky-Dresler et al., 1995**). Many studies have been made on the effect of process conditions and the following principles are obtained for the development of (111) recrystallization texture (**Tsunoyama, 1998**):

1. increasing coarseness of precipitates in hot bands;
2. decreasing grain sizes of hot band;
3. increasing cold reduction rate;
4. increasing annealing temperature.

However, these studies are not sufficient to make clear the mechanism of (111) texture development.

Thus, it is important to have a thorough understanding of the underlying physical metallurgy involved so that the desired recrystallization texture is obtained by suitably controlling the prior processing steps to result in formable grade of steels.

3. Processing of aluminium killed EDD steels

In annealed EDD, three types of microstructures are possible depending upon the stage while AlN precipitate forms from Al & N in solid solution (Auburn & Rocquet, 1973):

i. equiaxed grain structure is obtained while AlN either forms during coiling or after recrystallization during annealing.
ii. The transition zone recrystallized microstructure forms while recrystallization and AlN precipitation occur simultaneously.
iii. elongated or pancake grain structure is obtained while AlN forms prior to recrystallization during annealing. The AlN precipitates form on the defects of cold rolled structure and thus, recrystallization is retarded. A remarkable enhancement of {111}<uvw> crystallographic orientation occurs as nucleation occurs more rapidly in grains of this type (**Beranger et al., 1996**)

EDD steel sheets are produced by either batch or continuous annealing of cold-rolled steel sheets containing carbon up to about 0.05% and Mn up to about 0.2% (**Sarkar et al., 2004**). However, the physical processes involved in these processes are different. Thus, batch and continuous annealing processes will be detailed separately in the following sections.

3.1 Hot band texture

The hot band texture of such steels is reported to be nearly random with rotated cube component {001}<110> being approximately 2 times random (2XR) (**Heckler & Granzow, 1970**).The recrystallization of austenite during hot rolling is reasonably fast and gets completed prior to the transformation to ferrite. Further, in EDD steels no other texture component remains present after hot rolling indicating the fact that the austenite did not have any deformation texture component prior to transformation to ferrite (**Ray et al., 1990).**

3.2 Cold rolled texture

The cold reduction has an important role in dictating the grain morphology after annealing, texture and mechanical properties. **Figure 2a -2c** depict the effect of cold reduction on grain size, r_m-value (drawability) Δr (planer anisotropy—earing) for an EDD grade steel (C: 0.034%, Mn: 0.21%, Al: 0.06% and N: 0.005%) (**Hebert et al., 1992**). Thus, an optimized cold reduction must be taken into account while high deep drawability as well as minimum earing is desired.
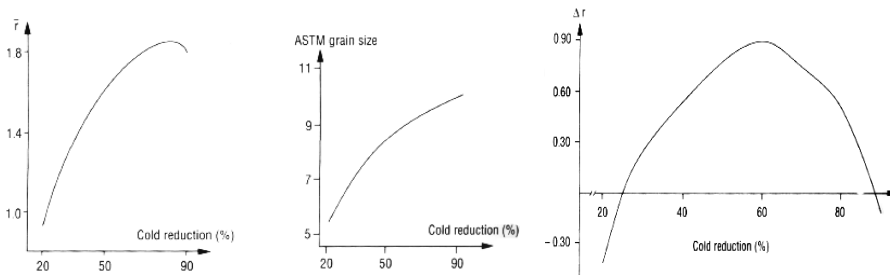
Fig. 2. (a) Variation of $\bar{r}$ (r_m-value) with cold work, (b) variation of grain size with cold work and (c) variation of Δr with cold work for the EDD grain steel (Hebert et al., 1992).

With increasing cold reduction the steel develops both partial α-fiber <110>||RD and γ-fiber {111} ||ND. The transformed {001}<110> component also strengthens noticeably. With the increase in cold reduction from 60% to 80%, the strongest texture component shifts from {111}<10> to {112}<110> (**Heckler & Granzow, 1970**)

3.3 Batch annealing

Since the pancake grain structure provides favourable texture for high deep drawability, the processing parameters are set to obtain pancake structure, while transition zone structure is avoided since the latter results coarse grains (ASTM<8) leading to reduced ductility and the risk of orange peel formation during drawing. In order to ascertain that the nitrogen remains in solution, the AlN that forms in the cast material requires to be dissolved during slab reheating (**Auburn & Rocquet, 1973; Meyzaud et al., 1974).** Usually, soaking temperatures of the order of 1200-1250ºC are necessary. In addition, the recombination of Al with N also needs to be prevented during cooling and coiling after hot rolling. To attain this, the finish rolling temperature must be high enough and above Ar3 **(Figure 3) (Beranger et al., 1996)** followed by fast cooling in the AlN precipitation range in association with low coiling temperature (<600ºC), **Figure 4 (Beranger et al., 1996**) to avoid poor ductility and drawability in the annealed steel.

3.4 Continuous annealing

Continuous annealing lines combine several processes including cleaning, annealing, over aging or galvannealing, and sometimes temper rolling, in one continuous operation. In continuous annealing due to high heating rate, recrystallization during annealing occurs at higher temperature than batch annealing and the precipitation of AlN occurs after recrystallization with nitrogen previously in solution. Thus, the nucleation of preferred oriented grains is hindered and due to nitride precipitation, subsequent growth of the recrystallized grains is also restricted. This causes the development of unfavourable texture. Further, the presence of carbides and carbon in solution during recrystallization also assist in the formation of unfavourable texture for drawing.
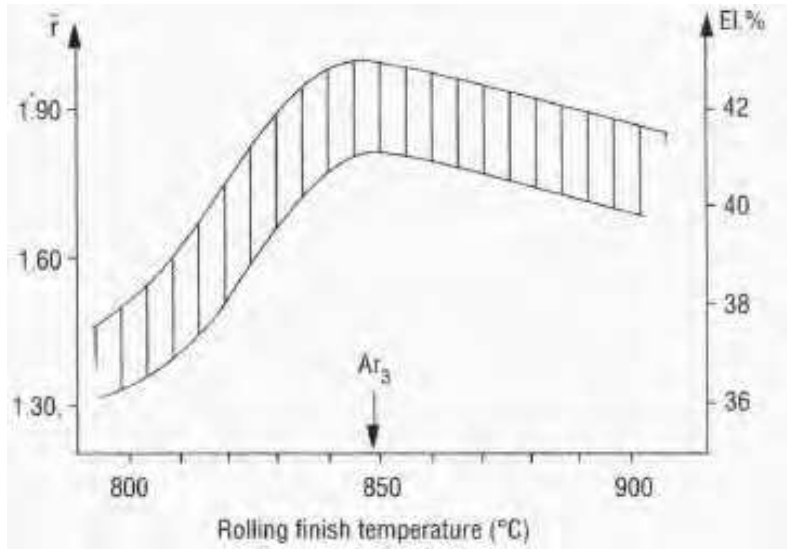
Fig. 3. Variation of $\bar{r}$ (r_m-value) and ductility with finish rolling temperature for a batch annealed EDD steel (**Beranger et al., 1996**).
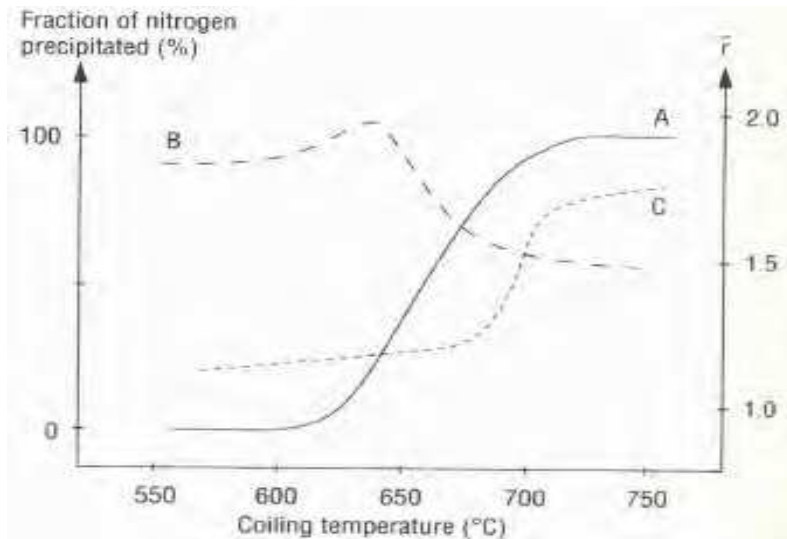

Fig. 4. Variation with coiling temperature of (A) AlN precipitation,(B) the r_m-value in batch annealing and (C) the r_m-value in continuous annealing for a low carbon low manganese EDD steel.(Beranger et al., 1996).

Therefore, in continuous annealing it is endeavoured so that AlN is precipitated prior to annealing, by high temperature coiling after hot rolling. Otherwise, by reheating the as-cast slabs at a temperature too low to take the nitrides back into solution.

However, high temperature coiling has two disadvantages (**Beranger et al., 1996**):

- It causes variation in mechanical properties in the product due to difference in cooling rate between middle and end regions of the coil. A selective coiling technique in which coiling the ends at higher temperature is performed can reduce the property heterogeneities.
- May cause abnormal grain growth for a certain combination of finish rolling and coiling temperatures which causes defect in both hot and cold rolled sheets.

Thus, to obtain favourable texture and improved deep drawability and therefore, to increase annealed grain size, it is required that the rate of nucleation of recrystallized grains is reduced, which can be done by lowering of recrystallization temperature. This can be achieved by (i) reducing the carbon content, alloying elements and impurity elements and (ii) increasing the stored energy of deformation by higher cold deformation, adjusting the composition or hot rolling parameters to obtain desired distribution of hot band precipitates (**Lebrun et. al, 1981**) .Control of the dissolved carbon and carbide contents is achieved by lowering the carbon content of the steel, overageing after continuous annealing, coarsening of the cementite particles and reducing the rate of redissolution of the carbides during annealing. High temperature coiling also promotes coarsening of the carbides present.

Thus, contrary to batch annealing high temperature coiling improves texture and drawability for EDD steel in continuous annealing (Figure 4). In batch and continuous both, a temper rolling is recommended after annealing to remove yield point elongation and thus to avoid stretcher strains in the final product.

4. Recrystallization texture and formability for EDD steel

4.1 Heating rate effect

While the Al and N are kept in solution prior to annealing, the microstructure varies with heating rate and mechanical properties and r_m-value are strongly dependent on heating rate during annealing as represented by **Figure 5 (Beranger et al., 1996)**. Batch annealing involves placing sheet steel coils in a gas fired furnace with a controlled atmosphere. Batch annealing cycles normally involve slow heating up to about 700 ℃. Slow heating after cold rolling is normally necessary to allow adequate time for the Al to diffuse, forming clusters or precipitates before recrystallization commences. Thus, low heating rate leads to the precipitation of AlN during recovery that helps generate strong {111} texture after recrystallization. The precipitation of AlN takes place at a lower temperature and this is followed by recrystallization of the steel at a higher temperature (Takahashi & Okamoto, 1974). The optimum heating rate up to the precipitation stage to obtain highest r_m-value was calculated by Takahashi and Okamoto (**Takahashi & Okamoto, 1974**): Log (PHR) = 18.3 + 2.7 log((Al) (N) (Mn)/R_{CR}), where PHR is the peak heating rate in Kh^{-1} corresponding to the peak in r_m-value, (Al), (N) and (Mn) are solute concentration in weight percent and and R_{CR} is the percentage reduction via cold working. The holding temperature is always below Ac1 that varies in the range of about 650-720℃ (**Beranger et al., 1996**). The coils are then slowly cooled at 10℃/hour (Takahashi & Okamoto, 1974) and the process takes several days in batch annealing.
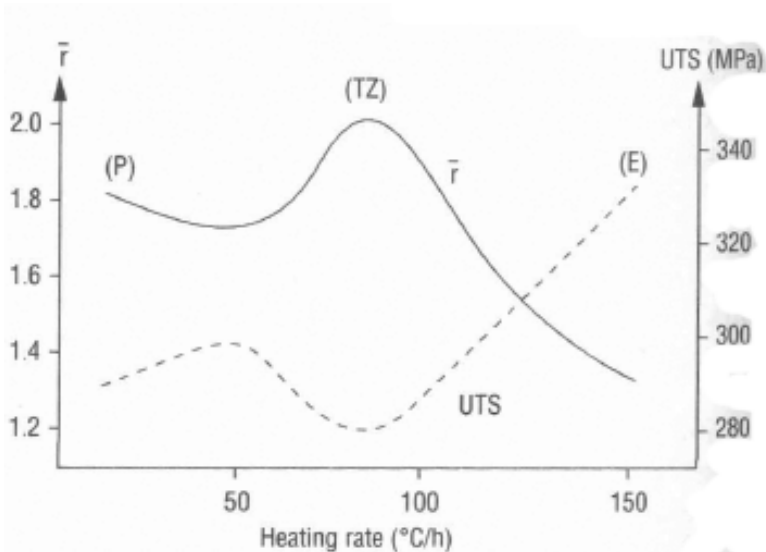
Fig. 5. Variation in r-bar (r_m) UTS values and microstructure with heating rate for batch annealed aluminium killed steel (Beranger et al., 1996).

Kozeschnik et al (**Kozeschnik et al., 1999**) calculated the logarithmic intensity ratio I_{111}/I_{100} at various annealing heating rates for the EDD steel. **Figures 6** (heating rate 50K/h) and **7** (heating rate -120K/h) show the effect of heating rate variation on the logarithmic intensity. Due to diminishing effective particle/recrystallization interaction time, the absolute value of the maximum intensity ratio is significantly decreased at higher heating rates. This effect is due to the shorter time available for aluminum nitride precipitation prior to the start of the recrystallization process. A higher supersaturation is needed in order to keep the two competing mechanisms balanced. Figure 8 shows the calculated variation of the I_{111}/I_{100} ratio with different heating rates. The qualitative comparison of the calculated logarithmic X-ray intensity ratios given in **Figure 8** and the experimental data for the r_m-value of Al-killed steel processed at low coiling temperature in Figure 9 (Hutchinson, 1984) shows good agreement.

Sarkar et al (**Sarkar et al., 2004**) also studied the effect of annealing heating rate on 70% cold rolled 0.05-C-0.19Mn-0.008 S-0.051Al EDD steel. In their work they selected heating rates of 50 and 70°C/h to the intermediate annealing temperatures of 550 and 600°C, and 15 and 30°C.h from intermediate annealing temperature to the final annealing temperature of 700°C. The soaking time at the intermediate and final annealing temperatures was half an hour. Tensile test and formability test inferred that the Annealing cycle that consisted of heating rate, 50°C/h to 600°C intermediate annealing temperature and 30°C/h up to 700°C resulted in the best combination of mechanical and formability properties with enhanced r_m of 1.92 and plane strain forming limit of 35%. The attractive combination of properties with high formability was attributed to the huge number of small spherical carbide precipitates that resulted in pure ferrite devoid of solute carbon.
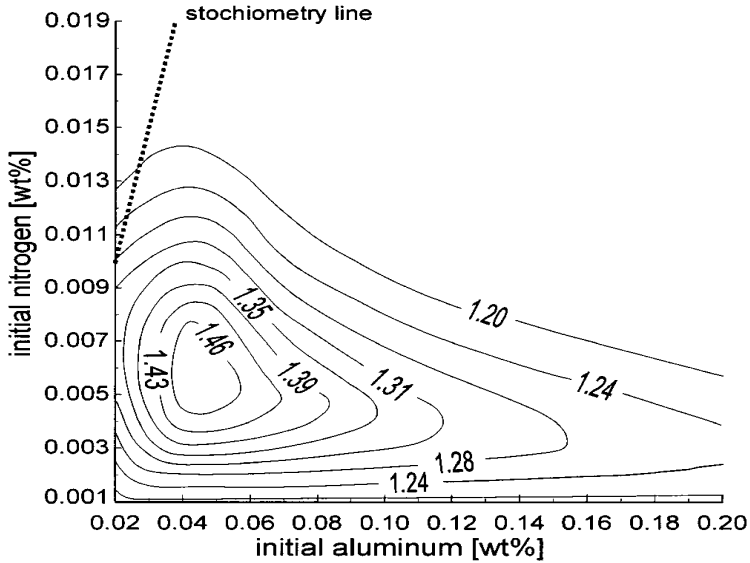
Fig. 6. Calculated logarithm of the intensity ratio (111)/(100) for a coiling temperature of 550 °C and a heating rate of 50 K/h as a function of initial amount of aluminum and nitrogen. [**Kozeschnik et al., 1999**]
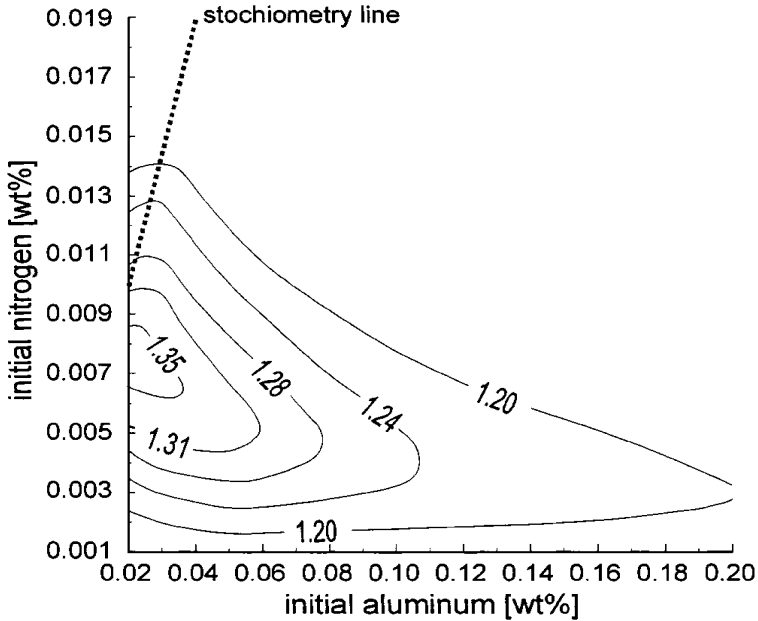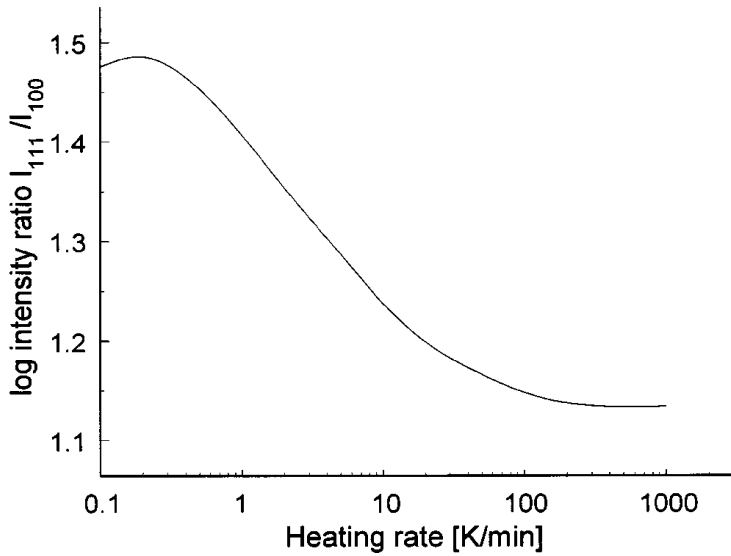

Fig. 7. Calculated logarithm of the intensity ratio (111)/(100) for a coiling temperature of 550 °C and a heating rate of 120 K/h as a function of initial amount of aluminum and nitrogen. [**Kozeschnik et al., 1999**]

Fig. 8. Calculated logarithm of the intensity ratio (111)/(100) as a function of the heating rate during annealing for Al_{solute} = 0.03 wt pct and N_{solute} =0.005 wt pct. **(Kozeschnik et al., 1999).**
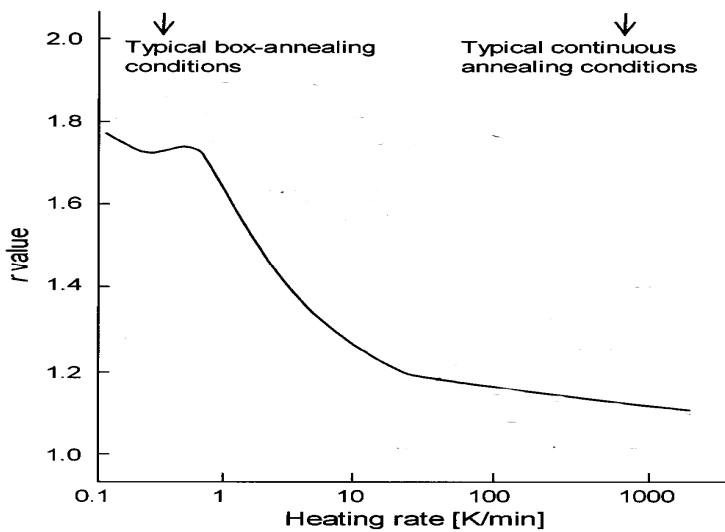

Fig. 9. Variation of mean plastic strain ratio, r_m with heating rate for EDD steel with low coiling Temperature (**Hutchinson,1984**).

4.2 Manganese and sulfur effect

Figure 10 (a, b) (**Ray & Jonas, 1990)** shows the comparison between the ODFs obtained from high Mn-high S (0.31%Mn, 0.018%S) and low Mn-low S (020%Mn, 0008%S) cold rolled batch annealed EDD steels, respectively. With the advances of steel making technology with desulphurization, the required Mn content to tie up with sulpher also reduced. The above technology in association with somewhat higher cold reduction, helped develop stronger γ-fiber (Fig 10b) that led to r_m, 1.8. While the r_m value obtained for the high Mn-high S steel (Fig 10a) was 1.5.

In the case of Al-killed steel, the optimized sheet properties are attained as a result of interaction between two processes: aluminium nitride precipitation and recrystallization (**Schulz, 1949**). Apart from pancaking of grains, the number distribution and morphology of carbides also play a role in formability. Smaller, spherical, and larger in number of carbides give good formability, because in this way the ferrite contains less C (ferrite is purer), which helps formability. Therefore, in order to improve the property of deep drawing sheet it is important to control every processing step effectively.
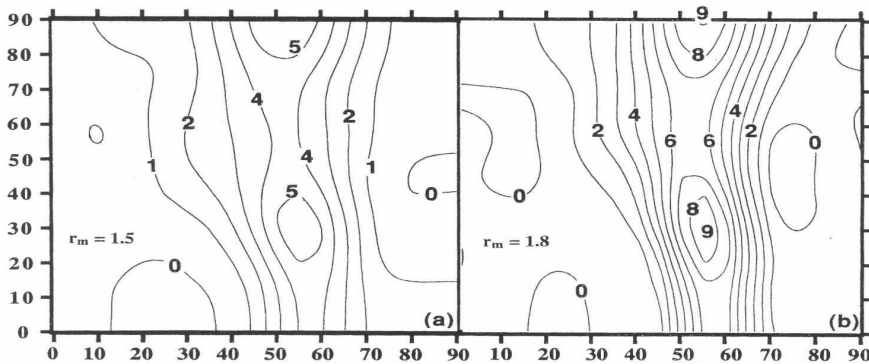

Fig. 10. $\varphi2 = 45°$ sections of CRBA EDD steels showing (a) the ODF for the high Mn high S (0.31%Mn, 3 0.018%S) steel and (b) the ODF for low Mn, low S steel (0.20%Mn, 0.008%S) (Ray & Jonas, 4 1990).

4.3 Chromium effect

Mendoza et al (**Mendoza et al., 2004**) developed a chromium stabilized EDD steel (C: 0.02, Mn: 0.2, Al: 0.04, Cr: 0.35) by electric arc furnace, vacuum degassing, ladle treatment and continuous casting route. The steel sheet after cold reduced by ~85% was isothermally annealed under a protective argon atmosphere and was annealed at 700 ∘C from 1 to 300 s. The heating and cooling rate of annealed sheet specimens were ∽10 and ∽80 ∘C/s, respectively.

Figure 11 shows the SEM-micrograph of the as-cold rolled specimen. As may be observed, the ferrite grains are flattened, and inside the grains some shear bands can be observed. These in-grain shear bands corresponded to the narrow regions of intense shear that carry large strains during deformation and appear to become the major deformation mode (**Park et al.,2000**). In some interstitial free-steels also, it was observed that in-grain shear bands

were inclined at angles of 30°–35° to the rolling plane (Barrett & Jonas, 1997). For instance, Barnett and Kestens (**Barnett et al., 1999**) reported that the increasing density and severity of these in-grain shear bands lead to a bulk recrystallization texture dominated by {1 1 1}<1 1 2> near the normal direction–rolling direction (ND–RD) for low carbon, ultra low carbon and interstitial free steels. In the present chromium stabilized EDD steel, the shear bands were inclined ∽32° with respect to the rolling plane and were almost parallel to each other within the individual grains.
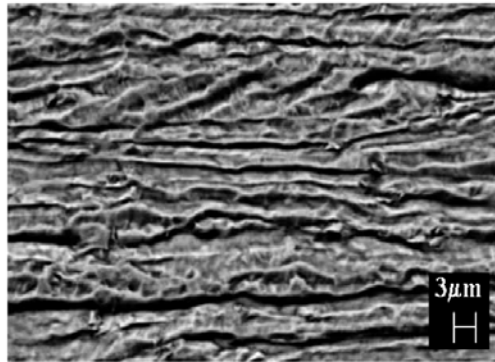

Fig. 11. Hot band microstructure of chromium stabilized EDD in hot rolled plates with flattened ferrite grains closely parallel to the sheet plane and inside the grains, some shear bands are observed (**Mendoza et al., 2004**).

Figure 12 shows {1 0 0} pole figures for the steel in the hot rolled, cold rolled and annealed conditions. It may be observed that in the cold rolled sheet, a {5 5 4}<2 2 5> component was noticed near {1 1 1}<1 1 2> texture. While, in the annealed sheet an appreciably strong texture than in the as cold rolled condition was observed from {5 5 4}<2 2 5> to {2 1 1}<0 1 1>. The microstructure obtained in the annealed condition was partially recrystallized, which was attributed to the presence of chromium-carbides precipitates that helped retard the recrystallization rate of the low carbon Al-killed/Cr-stabilized steel and which eventually was instrumental in the formation of {1 1 1}<1 1 2> textures.
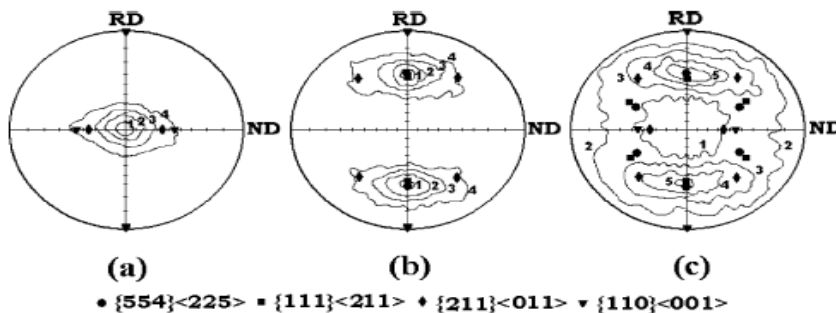

Fig. 12. {1 0 0} pole figures for the chromium stabilized EDD steel in (a) hot rolled, (b) cold rolled and (c) annealed conditions (**Mendoza et al., 2004**).

The mechanical properties of the annealed chromium stabilized EDD sheet are depicted in **Figure 13.** The use of chromium instead of niobium or titanium to stabilize the low carbon steel was effective in slowing down the recrystallization rate, thus, enhancing the formation of {1 1 1}<1 1 2> textures and achieving $\bar{r}$ values (r_m- values) >2 (Mendoza et al., 2004).

Fig. 13. Mechanical properties of annealed coils. (a) Hardness Rockwell b, (HRb), (b) 0.2% of yield strength, (YS), (c) tensile strength, (TS), (d) percent of elongation, (El), (e) the average plastic anisotropy value, ($\bar{r}$) and (f) the strengthening hardening exponent, n (**Mendoza et al., 2004**).

4.4 Phosphorous effect

It was observed by researchers that rimmed steel with P addition and by annealing the cold rolled sheet in decarburization furnace improved formability and thus studies were made on EDD steels to examine the interactive effect of P and AlN precipitation on formability of the steel sheets (Beranger., et al).

4.4.1 Heating rate effect on phosphorous added EDD steel

Rephosphorized Al-killed (EDD-P) steels show the similar dependence on heating rate of grains to conventional Al-killed steels (**Ono et al., 1982**). However, the smaller grain size, lower grain elongation ratio, lower r_m-value, faster recrystallizatio rate observed in the EDD-P steel were all attributed to the effect of phosphorous on the precipitation site of AlN. If phosphorus weakens the retardation effect of AlN on recrystallization, the restriction on nucleation of less favourable orientations, other than the {111} nucleus by AlN, which is usually observed in EDD steels will be relieved, resulting in the reduction of (111) intensity and an increase in the {100} intensity. In EDD-P steel {111}<112> orientation is observed unlike {111}<110> in the conventional EDD, which was attributed to the modification of cold rolled microstructure by phosphorous.

Figure 14 (Ono et al., 1982) shows the change in X-ray integrated intensity during heating. From the early stage to the half way of recrystallization, a rapid increase in the {222} intensity in association with a rapid decrease in the {200} and {110} intensities were observed in the EDD-P steel (Steel−1: C: 0.05, Mn-0.24, P:0.069) as well as in the conventional one (Steel-4: C:0.05, Mn:0.26, P:0.016). However, at the end of recrystallization, the EDD-P steel showed a lower {222} intensity and a higher {200} intensity than the conventional one. There was a marginal difference in the {110} intensity between them.

4.4.2 Manganese effect on phosphorous added EDD steel

An optimum combination of phosphorus and manganese content in steel can render a strong {111} texture through a simulated batch annealing cycle. As per Hu and Goodman (**Hu & Goodman, 1970)** and Hughes and Page (**Hughes & 1971)** the interaction between manganese and carbon would affect the recrystallization kinetics and thus, recrystallization textures. Further, Matsudo et al. (**Matsudo et al, 1984**) reported the detrimental effect of the Mn-C interaction on the drawability. On the other hand, it is widely known that steels containing phosphorus are likely to show a banded structure with segregated P-bearing ferrite, suggesting phosphorus and carbon in steel can act as repulsive elements to each other.
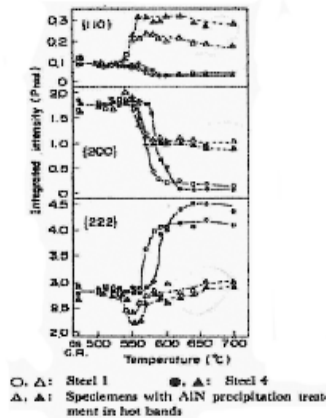
Fig. 14. Change in integrated intensity of Steels 1 and 4 during continuous heating at a peak heating rate 50°C/hr. **(Ono et al., 1982).**

Hu (**Hu, 1977**) reported that the drawability of low-carbon steel containing 0.067 pct P diminished more gradually than that of P-free steel with increasing manganese content up to 0.3 pct.

However, the work conducted by Chung et al (**Chung et al., 1987**) to examine the effect of manganese on the development of {111} recrystallization textures of P-containing low-carbon Al-killed steel sheet demonstrated that the phosphorous addition could modify the Mn-C interaction favourably for achieving improved drawability in EDD steels. **Figure 15** shows the (200) pole figures for the 0.1 pct P and P-free steels annealed at 973 K for 3 hours. The P-containing steels manifested {554} (225)-type texture and the texture was extremely

strong in the 0.78 pct Mn-0.1 pct P steel. On the other hand, in the P-free steels the texture was not as strong at 0.5 pct Mn as it was at 0.06 pct Mn.
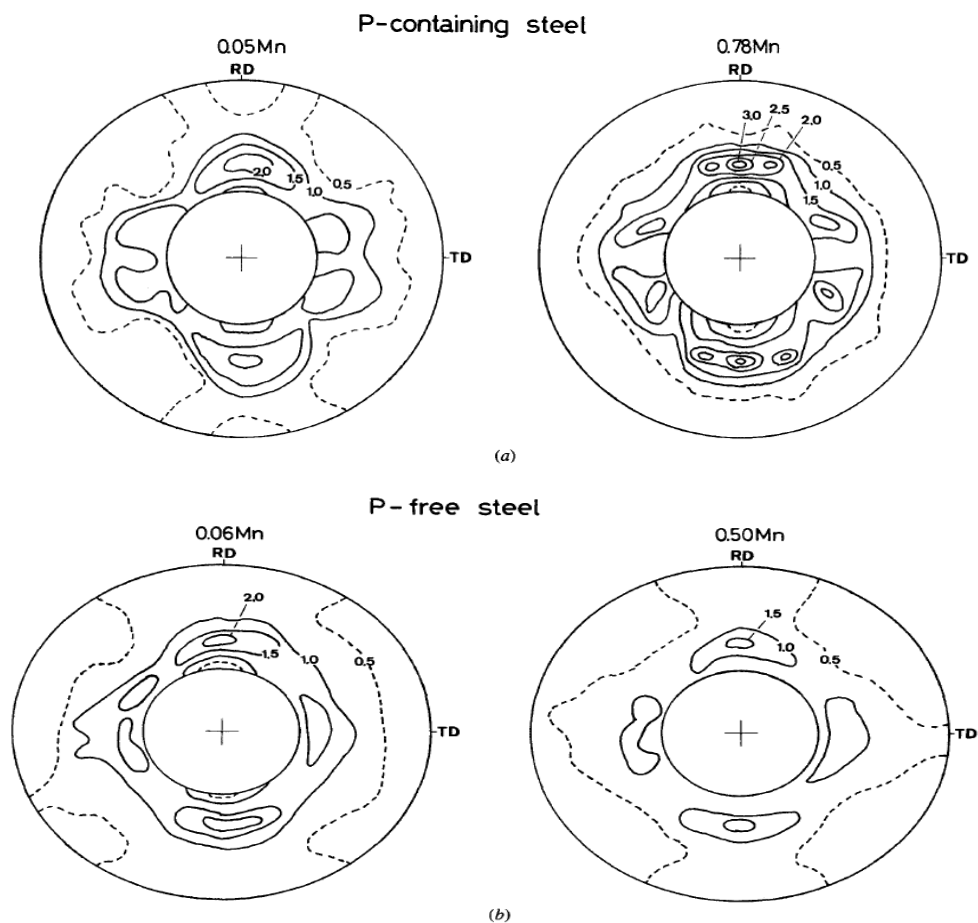

Fig. 15. (200) pole figures for (a) 0.1 pct P steels normalized, cold rolled, and annealed at 973 K for 3 h and (b) P-free steels normalized, cold rolled, and annealed at 973 K for 3 h (**Chung et al., 1987**).

To confirm the effectiveness of phosphorus addition to a high manganese steel in order to get a high r_m-value, the 0.2 pct P-1.2 pct Mn steel was employed. The recrystallization texture, as shown in **Figure 16**, had strong {554}(225) components which were favorable for a high r_m-value. The r_m-value and other mechanical properties are shown in **Table 1** (**Chung et al., 1987**). The high manganese P-containing steel had a tensile strength of 430 MPa and an r_m-value of 2.0.
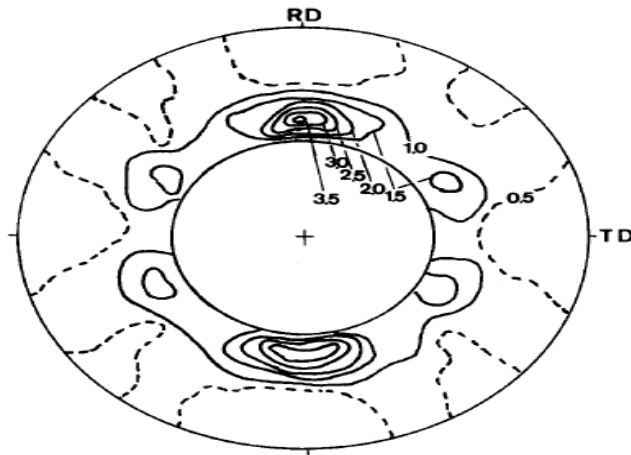
Fig. 16. (200) pole figure of 0.2 pct P-1.2 pct Mn steel preaged at 843 K for 24 h, cold rolled 75 pct, and annealed at 973 K for 4 h (**Chung et al., 1987**).

The micrographs of the P-free steel and the P-containing steel hot rolled and aged are shown in **Figures 17** and **18**, respectively. In the P-free steels, the precipitates that were identified as AlN dispersed within the grain at 0.06 pct Mn, whiles the precipitates were barely noticed at 0.5 and 1.0 pct Mn. On the other hand, in the P-containing steels, precipitates which might be $(FeMn)_3C$ and/or AlN were dispersed uniformly in the ferrite matrix only at the 1.5 pct Mn level. From the results, it must be noted that the fine precipitates of nitrogen and/or carbon disperse uniformly with decreasing manganese in the P-free steels, and vice versa with increasing manganese in the P-containing steels.
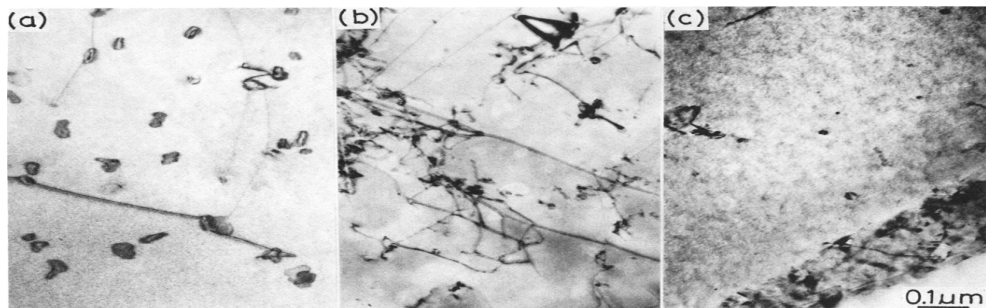
Fig. 17. Transmission electron micrographs of P-free Al-killed steels aged at 833 K for 1000 h after hot rolling. (a) 0.06 pct Mn, (b) 0.5 pct Mn, and (c) 1.0 pct Mn **(Chung et al., 1987).**
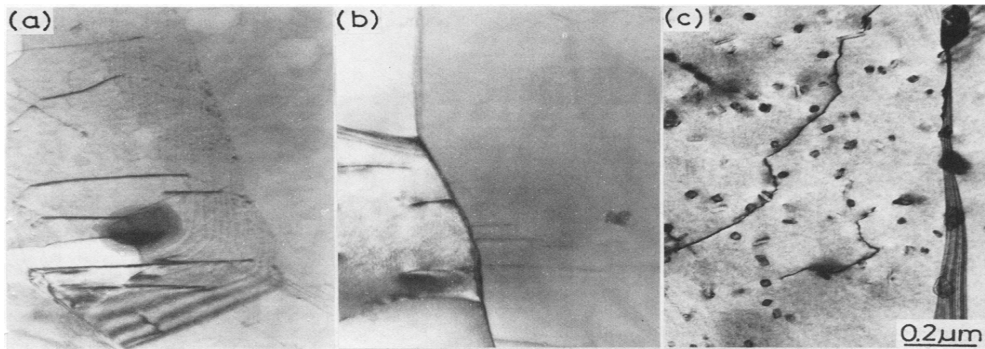
Fig. 18. Transmission electron micrographs of 0.2 pct P steels aged at 843 K for 24 h after hot rolling. (a) 0.1 pct Mn, (b) 0.5 pct Mn, and (c) 1.5 pct Mn **(Chung et al., 1987).**

Y.S. (MPa)	T.S. (MPa)	Uniform El. (Pct)	Total El. (Pct)	r_0	r_{45}	r_{90}	$\bar{r}$
262	434	24	33	1.60	2.09	2.25	2.01

Table 1. Mechanical properties of 0.2 pct P-1.2 pct Mn Al-Killed steel preaged at 8543 K, cold rolled 75 pct, and annealed at 973 K for 4 hrs.

Thus, a strong recrystallization texture with {554} (225) texture component and an uniform dispersion of $(FeMn)_3C$ in ferrite matrix can be developed through batch annealing of a P-containing EDD- steel if the steels contain high P and high-Mn .

5. On metallurgy of ultra-low carbon interstitial-free (IF) steels

Interstitial free steels are highly formable due to their low carbon and nitrogen content of ((wt%) < 0.003% and < 0.004%, respectively). The C and N are tied to Ti, Nb etc as precipitates. A limited excess of titanium or niobium relative to carbon, nitrogen and sulfur contents has a favourable influence on mechanical properties. During hot strip rolling, the level of interstitial elements, such as C and N, remnant from the steel making process, can be reduced by combining them with the stabilizing elements. The application of these steels is in the rear floor pan, front, rear door inners, etc.

5.1 Titanium stabilized IF steels

Titanium is very effective in scavenging nitrogen, sulphur, and carbon, readily forming TiN during casting and TiS during slab reheating . Subsequently, while the nitrogen and sulphur are scavenged, remaining Ti ties up with TiC during coiling. The minimum amount of titanium required for full stabilization, based on a stoichiometric approach, is **(Tither & Stuart, 1995)**:

$$Ti_{stab} = 4C + 3.42N + 1.5S$$

It was proposed that excess Ti addition than that required to combine with all C, N, and S was beneficial to achieve high r values (**Gupta & Bhattacharya, 1990**). Excess Ti (Ti*) is given by :

$$Ti^*=Ti_{total} -(4C+3.42N+1.5S)$$

However, it is also commented that an excess Ti content can be linked to the incidence of surface streaking. The frequency of appearance of this type of defect can be minimized using Nb in combination with Ti. Titanium only intierstitial free steels are the least susceptible to compositional changes and process variation. This is attributed to the precipitation of Ti compounds at higher temperatures (TiN, TiS) that play less of a role in subsequent lower temperature processing (Krauss et al., 1991). Tsunoyama et al (**Tsunoyama et al, 1988**) considered three precipitation mechanisms suggested by various authors: a) TiS may provide a preferential site for TiC nucleation. Thus, lowering the S content can retard the precipitation of TiC b) with decreasing Ti content, precipitation of $Ti_4C_2S_2$ occurs in place of TiS and controls carbon stabilization. The stabilization of C by $Ti_4C_2S_2$ is preferred compared to TiC precipitation as $Ti_4C_2S_2$ precipitates are larger, remove solute carbon from the matrix earlier, and are more stable.

The precipitation mechanism of titanium in these steels is summarized in **Figure 19** (**Tither, 1994**). It is postulated that titanium nitride particles formed during slab casting acted as nucleation sites for the precipitation of TiS and $Ti_4C_2S_2$. The small amount of carbon remaining is precipitated as TiC. During reheating of the slab, solution of carbosulphide occurs, leaving only TiS and TiN. Cooling of the strip to the inctercritical (austenite -ferrite transformation) temperature region during hot rolling transforms TiS to $Ti_4C_2S_2$ by the absorption of titanium and carbon.

5.2 Niobium stabilized IF steels

In Nb IF steels, Nb forms carbonitride precipitates. The aluminium addition during the killing process also reacts with N to form AlN. However, the favourable solubility product of AlN compared to NbCN, leads to preferential precipitation of AlN at a higher critical temperature. This reduces the N available for the precipitation as NbCN. The solubility products are dependent on bulk chemistry, temperature, and precipitate composition. The precipitates sequence in such steels can be considered as (**Holie, 2000)**

$$Al+N=AlN$$

$$Mn+S=MnS$$

$$Nb+C+N=NbC$$
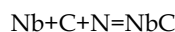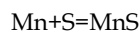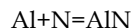
The solute Nb on grain boundaries introduces site competition for the elements like phosphorous, which enables lower ductile to brittle transition temperatures, poorer elongation and r_m- values than Ti IF steels. The niobium steels have higher recrystallisation temperature (750 - 800°C) than titanium stabilized IF steels (**Baker et al., 2002**) and it was reported that the temperature of recrystallisation of Nb IF could be up to 50 K higher than that of the Ti IF steels. This in turn requires higher finish rolling and annealing temperatures. The higher recrystallization temperature is attributed to the low temperature

formation of niobium carbides, producing fine particles that readily retard grain boundary movement during annealing.(**Tsunoyama, 1990**). The temperature can be reduced by lowering C content. In addition, recrystallisation temperature can be reduced to enhance drawability, using higher coiling temperature, so that precipitates are coarsened and subsequent pinning effect is reduced.
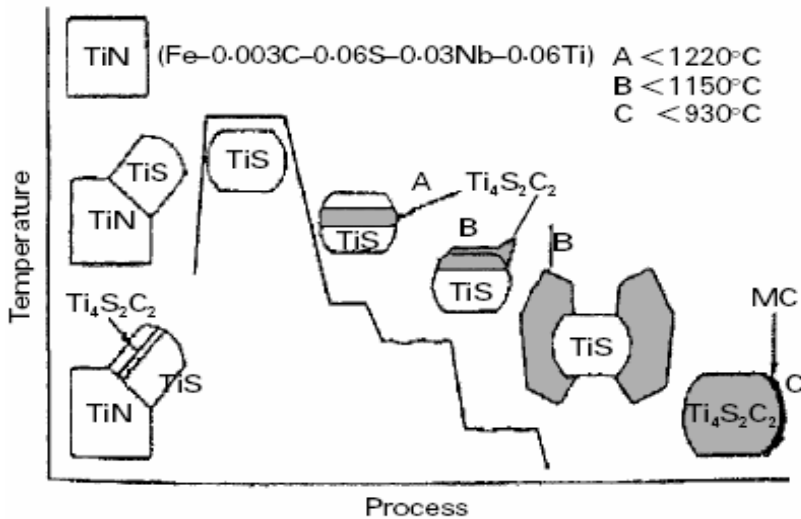

Fig. 19. Schematic mechanism of carbosulphide and carbide formation in titanium stabilized IF steels (**Tither et al., 1994**).

5.3 Titanium and niobium stabilized IF steels

Titanium in association with niobium added IF steels have the advantages of both Ti only and Nb only IF steels with reduced disadvantages. This combination provides the best combination of properties (**Tokunaga 1990**). The levels of Ti and Nb additions that are required to stabilize Ti +Nb IF steels are given by (**Holie, 2000; Tokunaga & Kato, 1990**)

$$(\%Nb)-(7.75(\%Ti)-3.42(\%N)-1.5(\%S))/4=0$$

If insufficient Ti is added such that the level of addition falls below that required for stabilization, TiN forms first and any S that is left behind after the formation of TiS is consumed as MnS. If the steel is understabilised by the insufficient addition of Ti and/or Nb then excess C exists in solid solution and a bake hardenable steel may be produced.

For IF steels, the increase in r_m-value with degree of cold work is continuous over the whole range employed in industrial production (**Beranger et al**).An increase in annealing temperature and/or holding time improves the deep drawability due to grain growth and recrystallization texture enhancement. Further, these grades have very high Ac1 temperatures, enabling continuous annealing at temperatures of ~850°C, or even higher. For such steels, the metal has no yield point elongation and no requirement of overaging treatments in continuous annealing, due to the absence of interstitials C and N.

5.4 Phosphorous effect on IF steels

One of the ways of increasing the strength of the IF steels is addition of solid solution strengtheners viz. P, Si and Mn to the steel (**Rege et al., 2000**). It has been found that P is the most potent and cost effective solid solution strengthener that increases strength without appreciably affecting the drawability of the steel (**Katoh et al., 1985; Tokunaga & Kato, 1990**). Mn, on the other hand, significantly deteriorates drawability and ductility (**Irie et al. 1981; Katoh et al., 1985; Tokunaga & Kato, 1990**), and Si adversely affects coating adhesion (**Nishimoto et al., 1982**). Thus, P is the preferred addition to increase the strength of IF-steel. However, it is found that phosphorus tends to segregate at the grain boundaries or precipitate out of the matrix during the recrystallization annealing. The phosphorus segregations reduce the cohesive strength of the grain boundaries, which leads to the secondary cold work embrittlement (CWE) and reduces the resistance of the steel to brittle fracture or more precisely, intergranular fracture (**El-Kashie et al. 2003; Rege & DeArdo, 1997**). The CWE is defined as the susceptibility of the sheet material to intergranular fracture during the secondary work of deeply drawn part or while in service. Cao et al (**Cao, 2005**) had reported that the segregation of phosphorus occurred when the P>0.07 wt pct in the IF steel. It is also found that the batch annealing leads to the higher phosphorus than the continuous annealing. The segregation behavior of phosphorus in the Ti and Ti+Nb IF steels was studied by Rege et al (**Rege et al., 2000**). It was found that the segregation of phosphorus to the ferrite grain boundaries occurred not only during the coiling stage of the thermo-mechanical processing, but also during the cold rolling and annealing process. The steels with higher phosphorus content showed higher ductile to brittle transition temperature, i.e, lower resistance to cold work embrittlement (CWE). The problem of CWE is more often encountered while annealing time is long, which enables P to segregate in the grain boundary (**Yasuhara, 1996**).

The CWE can be avoided by :

- controlling the chemical composition—i. e. by partial stabilization of carbon in IF steels or by addition of B/Nb - It is believed that P and C both segregate to the grain boundary and compete for the available sites, and C reduces the grain boundary segregation and embrittlement by P. Furthermore, C enhances the grain boundary cohesion and counteracts the embrittlement this way. B also plays the same role as that of C. Hence P-C or P-B site competitive process was expected to minimize the CWE phenomena. In Nb added steel it is believed that CWE is lower than that in Ti-stabilized steel that has been attributed to the partial stabilization of C in Nb-containing steel.
- grain boundary engineering—i. e. by grain boundary character distribution—by suitable annealing cycles low angle and low -CSL boundaries can be produced by avoiding the development of continuous random boundary network and which help reduce CWE.

6. Recrystallization texture and drawability of IF steels

Cold rolling plays an important role in the formation of favourable textures for deep drawing during annealing, however, has little effect on other properties. The variation of r-value with cold reduction in the three common IF steel types, Ti-stabilized, Nb-stabilized and Ti-Nb stabilized is shown in **Figure 20** (**Tokunaga & Yamada, 1985**). Ti -

Nb steels show the highest r-value for equivalent cold reduction. This was attributed to the fact that the precipitates formed during hot rolling and coiling were not large enough to compromise the r-value during annealing. A reduction of 90% produced the highest r-value in all the steels, however, these reductions were rarely achieved in practice, 80% being more common.
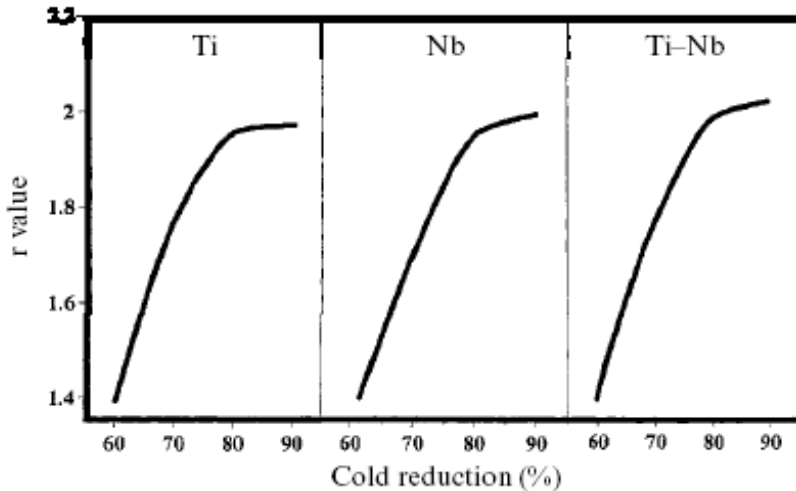

Fig. 20. Effect of cold reduction on r-value for titanium, titanium-niobium, and niobium IF steels (**Tokunaga & Yamada, 1985**).

Mendoza et al (**Mendoza, 2000**) studied the hot rolled precipitation behaviour of Ti-stabilized IF steels and mechanical properties and reported about improved r_m-value of 2-2.14. While Banerjee et al (**Banerjee et al., 2008**) vividly studied the precipitation of hot-band and annealed Ti stabilized IF steels to optimize hot and cold spot temperatures during annealing for improving drawability of the steels to >1.9. The hot bands of the as-received steels showed two types of texture development: (a) shear texture, manifested by {225}<554>, {110}<100>, and {113}<332> and (b) cold deformation type texture with a strong and incomplete α- fiber consisting of the components {001}<110>, {112}<110>, and {111}<110>, and the γ-fiber components, {111}<110> {111}<112>. The presence of a substantial amount of coarse equiaxed ferrite grains at the surface and finer grains at the central region was attributed to the outcome of finish rolling in the two-phase α+ γ region. On the other hand, the deformed grains at the surface and finer grains at the central region another hot band was the result of rolling in the single- phase α region. Figure 21 (Banerjee 21 et al., 2008) shows the φ2= 45o orientation distribution functions for various combinations of cold reduction and batch annealing temperatures to obtain improved r_m-value in an optimized processing condition. The poor texture and r_m-values at the annealing temperature of 660 oC were associated with the precipitation of fine precipitation of FeTiP-type within the grains and at the grain boundaries. This study had shown that for the given chemical composition of the Ti-IF steel, the optimized condition for cold spot temperature in batch-annealing cycle was 680 oC, preceded by 80 pct cold reduction, which resulted in an r_m-value of as high as 2.29.

The influence of the texture development in Ti-added (0.03, 0.05 and 0.07 wt%) IF on r_m-value was investigated by Kim et al (**Kim et al., 2005**). It was intended to determine the optimized Ti content for the promotion of deep drawability in the IF steels. For the IF steel with the composition of 0.0025C, 0.070Mn, 0.002N and 0.007S, the optimum Ti content was found to be 0.05wt%.

Juntunen et al (**Juntunen et al., 2001**) investigated the continuous annealing parameters in laboratory scale on drawability of Ti+Nb stabilized IF and IF-HS steels and it was reported that r_m-value could be enhanced by about 13% simply by adjusting the annealing conditions. The annealing cycle with maximum studied temperature produced the sharpest γ-fiber and highest r_m-value. While, Ruiz-Aparicio et al (**Ruiz-Aparicio, et al., 2001)** studied the evolution of the transformation texture in two $Ti_4C_2S_2$-stabilized interstitial-free (IF) steels (Ti and Ti/Nb) as a function of different thermomechanical processing parameters. Analysis showed that the $Ti_4C_2S_2$-stabilized steels stabilized were not very sensitive to the processing conditions employed in the study. The study also revealed that, under conditions of large deformations and coarse austenite grain sizes, the main components of the transformation textures are the beneficial {111}||ND orientations.
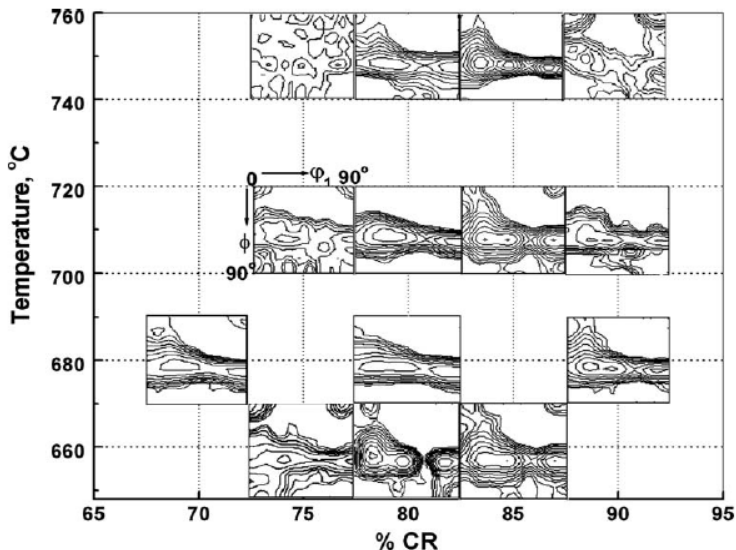
Fig. 21. ODFs of φ2 = 45º section at various processing conditions for a particular batch annealing temperature at various cold reductions. Maximum intensity for **660 ºC**: 75 pct-3.53, 80 pct -8.43, and 85 pct-6.43; for **680ºC** (hot spot): 70 pct-9.68, 80 pct-12.13, and 90 pct-10.38; for **710 ºC**: 75 pct-2.95, 80 pct-8.09, 85 pct-6.89, and 90 pct-4.13; and for 750 ºC: 75 pct-2.0, 80 pct-10.77, 85 pct-9.46, 90 pct-3.32 (**Banerjee et al., 2008**).

The effects of electric field annealing on the development of recrystallization texture and microstructure in a Ti+Nb stabilized cold rolled IF steel sheet were studied by He et al (**He et al., 2003**) means of ODF analysis and optical microscopy to assess the drawability response of the steel. Specimens of size 50 mm X 20 mm were cut from the sheet with the

longitudinal direction parallel to the rolling direction. They were then subjected to isothermal annealing at different temperatures ranging from 650 to 800 ºC for 15 min, respectively with or without a DC electric field of 200 V/mm. The annealing treatments were done in a nitrogen atmosphere and at a heating rate of 5 ºC/min to the chosen peak temperatures. The external electric field was applied by placing the specimens (positive electrode) in the middle of two parallel stainless steel sheets (negative electrode) that were 2 cm apart. The experimental arrangement is shown in **Figure 22**.
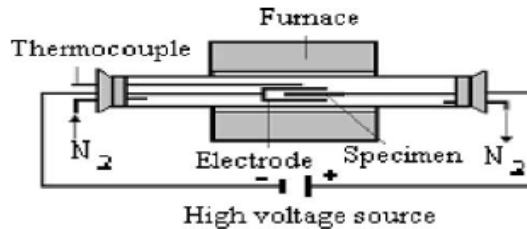
Fig. 22. Experimental arrangement for annealing with electric field (**He et al., 2003**).

Heating rate annealing experiments were carried out by Muljono et al (**Muljono et al., 2001**) to study the effect of heating rate on the recrystallization kinetics, grain size and texture of steels with a range of carbon levels (0.003–0.05% C). The steels were cold-rolled to 70% reduction and subsequently annealed at heating rates from 50 to 1000°C/sec to temperatures in the range 600 to 900°C. **Figure 23** shows that, for the 0.02 and 0.003% C steels, the {111}||ND texture increases in strength with increased heating rates up to 200°C/sec and maintains a plateau thereafter. Both steels exhibit similar trends and only the relative strength of the γ-fibre differs. The grain size and texture results are in general agreement with work by Hutchinson and Ushioda (**Hutchinson & Ushioda, 1984**). The {111}||ND components of the recrystallization texture increased at rates up to 200°C/sec due to enhanced nucleation at grain boundary sites.
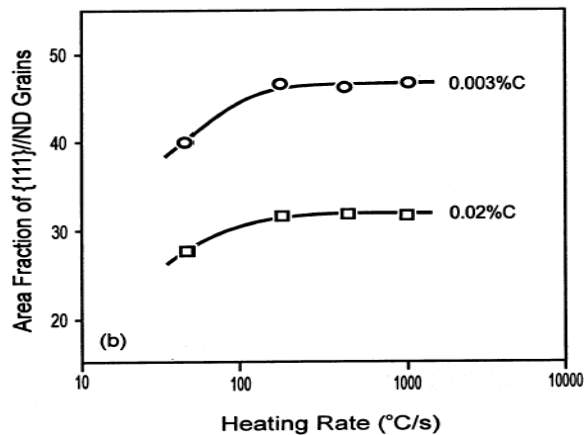

Fig. 23. Effect of heating rate on strength of recrystallization texture, given as the area fraction of grains within 15° of{111}||ND (**Muljono et al., 2001).**

During electric field annealing, specimens work as anode and the applied electric field reduces the lattice defect energy by lowering the shield effect that would decrease the driving force for recrystallization (**Cao et al.,1990; Conrad, 1989; Wang, 2000**). Thus, although the application of electric field generally reduces the driving force for nucleation and grain growth, the nuclei with random orientations are much more restricted than that of the γ-nuclei. Consequently, the electric field annealing yields a high nucleation rate for the γ-nuclei that lead to a relatively strong γ-texture after complete recrystallization. From Figures 24 and 26 (**He et al, 2003)** it can be noted that both kinds of specimens annealed with and without application of electric field, exhibited a similar tendency in the development of recrystallization textures, i.e. the α-fiber was weakened and the γ-fiber was strengthened with increasing annealing temperature. In addition the Figures 4 & 6 also depict that the application of electric field (200 V/mm) during annealing may promote the development of the γ-fiber (ND||<111>) recrystallization texture of the cold-rolled IF steel sheet, which is beneficial to the deep-drawability. While, Figures 25 and 27 (**He et al, 2003)** indicate that the recrystallization was noticeably retarded intensively by electric field annealing under the investigated conditions.
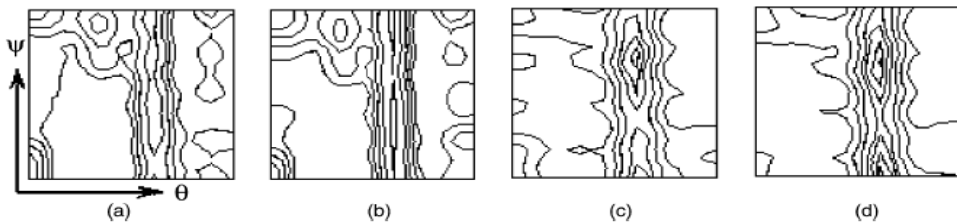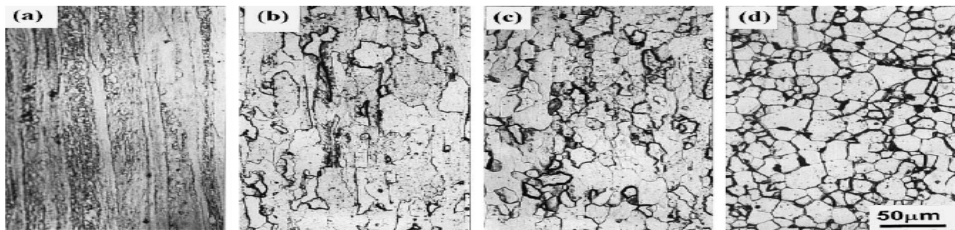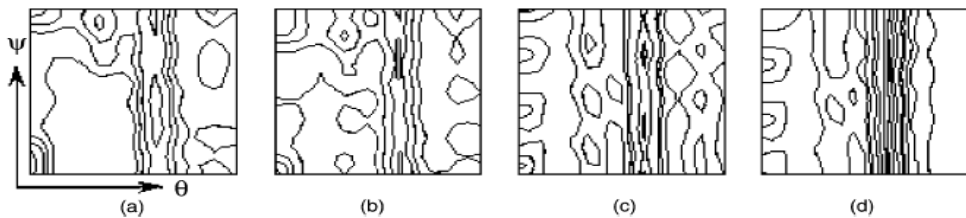

Fig. 24. φ= 45º sections of the ODFs (levels: 1; 2; 3; . . .) for the specimens annealed without an electric field at (a) 650 ºC, (b) 700 ºC, (c) 750 ºC and (d) 800 ºC (**He et al, 2003**).

In an innovative finding, Jeong communicated (**Jeong, 2000**) that r value was markedly improved by reducing the carbon content from 0.0035 (Steel B) to 0.0009 pct. (Steel A) in Ti stabilized IF steels that were treated with 0.25 pct Si, 1.25 pct Mn, and 0.09 pct P to attain tensile strength of 400 MPa (**Figure 28a**). The difference in r_m-value between two steels is 0.2 to 0.3 at all annealing temperatures (**Figure 28b**). Steel A containing 0.0009 pct carbon showed a high r_m-value of about 1.6 while annealed at 800 ºC to 860 ºC, corresponding to deep drawing quality (DDQ). The r_m-value increased to 1.85 for extra deep drawing quality (EDDQ) grade with increasing annealing temperature to 890 ºC. It was thus a remarkable finding as the steel was high strength steel with tensile strengths of 400 MPa or higher. This result indicated that while the carbon content decreases below 0.001 pct, superior formability of EDDQ grade could be achieved in high strength steel with tensile strength of 400 MPa or higher.

The highest $\bar{r}$ (r_m-values) in steels A and B were obtained in the specimens annealed at 890ºC while the coarsening of the ferrite grain was remarkable (**Figure 28c,d**). In order to find out the reason for the effect of carbon on the r_m-value, (200) pole figures for the annealed sheets were measured. The comparison of (200) pole figures of steels A and B showed that with the decrease in the carbon content, {554}{225} near the ND//(1l1) texture became stronger that was responsible for the improvement of r_m- value (Jeong, 2000).

Song et al (**Song et al., 2010**) worked on phosphorous segregation and phosphide precipitation on grain boundaries in association with drawability of rephosphorised IF steel .The cold rolled steel was annealed at 810ºC for 90 to 600 sec in a protected environment. The **Table 2 (Song et al., 2010)** illustrates yield strength, tensile strength and r_m-value reduce while n (work hardening index) value increases with the annealing time from 180 to 600 s. The phosphorus concentration at grain boundary is shown in **Figure 29** (**Song et al., 2010**). It was observed that as annealing time increased, the phosphorus concentration increased from 0.22 to 0.8 wt pct. The phosphorus concentration at the grain boundary is 20 times higher than that in the matrix for the sample annealed for 600 s, which greatly reduces the steel strength.

Fig. 25. Microstructures of the specimens annealed without an electric field at (a) 650 ºC, (b) 700 ºC, (c) 750 ºC and (d) 800 ºC (**He et al, 2003)**

Fig. 26. ϕ= 45º sections of the ODFs (levels: 1; 2; 3; . . .) for the specimens annealed with an electric field at (a) 650 ºC, (b) 700 ºC, (c) 750 ºC and (d) 800 ºC (**He et al, 2003**).
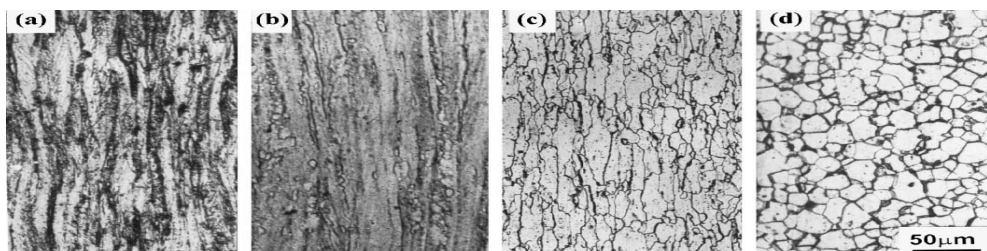

Fig. 27. Microstructures of the specimens annealed with an electric field at (a) 650 ºC, (b) 700 ºC, (c) 750 ºC and (d) 800 ºC (**He et al, 2003**).
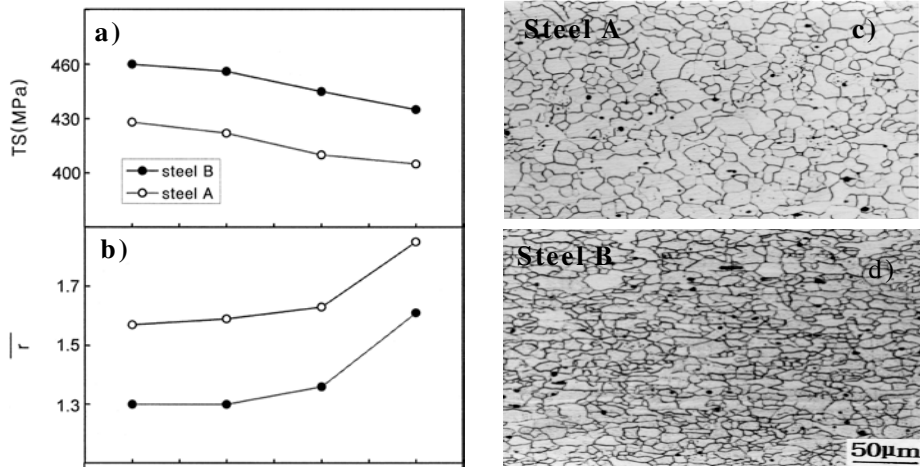
Fig. 28. Effects of carbon and annealing temperature on (a) tensile strength (b) $\bar{r}$ (r_m-value) and (c) & (d) ferrite grain sizes after annealing at 890°C for Steels A and B (**Jeong, 2000**).

Annealing time/s	Yield strength/MPa	Tensile strength/MPa	r	n
180	158.1	354.9	2.098	0.2376
360	155.4	346.8	1.939	0.2936
600	141.1	322.7	1.688	0.3046

Table 2. Mechanical properties of the annealed samples for different times
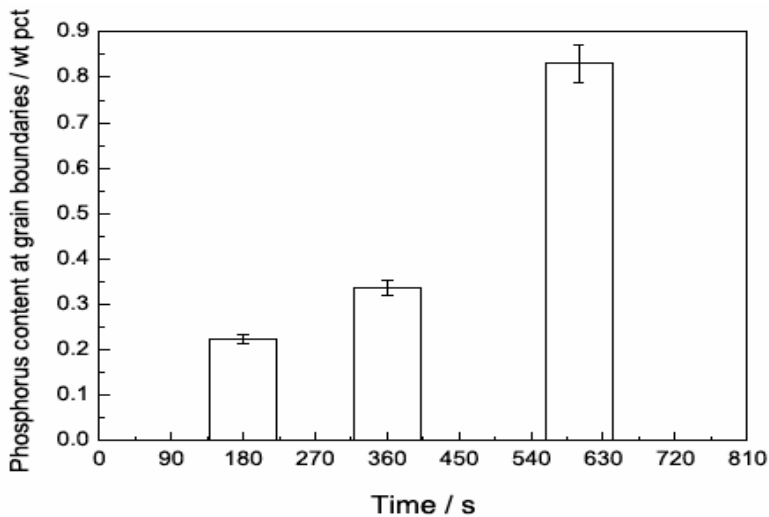
Fig. 29. Phosphorus content at grain boundaries in the rephosphorised IF steels annealed for different time 5 (**Song, et al., 2010**)

Kang et al **(Kang et al., 2007)** studied on the effects of aluminium on interstitial free high strength steel for the improvement of drawability (**Figure 30**). 78%cold rolled samples were annealed in an infrared-ray heating furnace. The annealing cycle consisted of heating the specimens to 830°C at a constant heating rate of 7°C/s and held at temperature for 30 s and then cooled to RT. Aluminum content more than 0.10 wt% improved the formability of the IF-HS. Texture analyses showed that the {111}||ND fiber (γ-fiber) was intensified, and <110>||RD (α-fiber) was weakened, with the increase of aluminum content. Recrystallization was completed earlier in the steel with the high aluminum content and the grain size of the annealed sample was larger than the steel containing lower aluminium. It was confirmed thorough the SANS analysis that the size of the precipitates in the sample with higher aluminum content was larger and their number was much fewer than in the sample with lower aluminum content. It appears that the high aluminum content in IF-HS containing Mn, P, Ti and Nb improved the scavenging effect of Ti or Nb and thus purified the iron matrix.
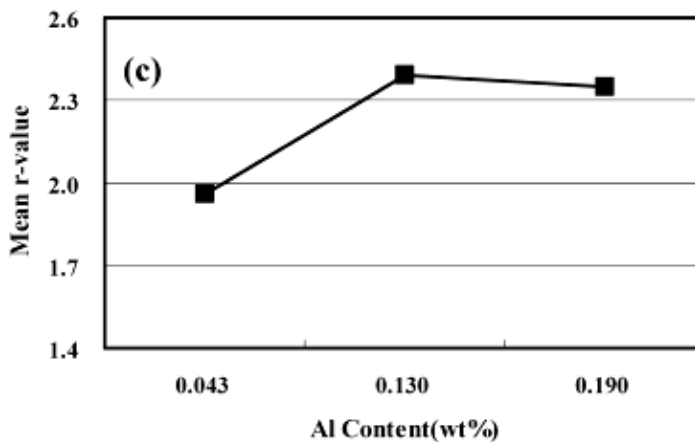

Fig. 30. Effect of aluminum content on mean r-value of the interstitial free high strength steel containing Mn, P, Ti and Nb (Kang et al., 2007) (**Kang et al., 2007**)

7. Metallurgy of bake hardening steels

Bake hardening is a diffusion controlled process involving the migration of solute carbon atoms within the iron lattice. The diffusion of these atoms is affected by heat treatment time and temperature and the amount of solute present in the steel. Factors such as grain size and dislocation density may also have an influence.

7.1 Mechanism of bake hardening

The yield strength increase from bake hardening is accompanied by the return of the yield point and yield point elongation; there may also be a slight increase in tensile strength and decrease in elongation. To attain such increased strength, the following criteria must be met: (**Matlock et al., 1998**)

i.   mobile dislocations must be present in the steel.
ii. there must be sufficient concentration of solute in the steel to pin these dislocations.
iii. the solute must be mobile at the aging temperature.
iv. dislocation recovery must be sufficiently slow to prevent softening.

The driving force for pinning is a reduction in lattice energy. Both impurity atoms and dislocations induce lattice strains in the iron matrix and these strains can be relaxed if the interstitial atoms diffuse to the vicinity of dislocations (**Mizui et al., 1990**).Bake hardening steel is amply used by the automotive industry for the outer panel of cars. This steel grade is characterized by low yield strength prior to final manufacturing process and a remarkably enhanced yield strength of the finished product in association with excellent deep drawability. The increase in yield strength during bake hardening of steel occurs due to the blocking of otherwise mobile dislocations by forming Cottrell atmosphere of solute carbon or iron-carbide precipitates during the baking operation after painting at 170ºC for about 20 minutes (**Kozeschnik et al., 1999**).

There are several types of bake hardening steel in production today. Individual grades are determined by the processing technology available and the properties required in the final product. These steels can be loosely grouped into two main categories, bake hardening EDD (aluminium killed) steels and bake hardening IF steels.

7.2 Bake hardening EDD steels

The EDD steel grades contain carbon content of the level~ 0.01%. If the carbon is allowed to remain in solution, room temperature aging occurs. Thus, carbon levels must be controlled by suitable annealing practices. These steels can exhibit problems during galvannealing, however, their main disadvantage is poor formability due to the presence of relatively high carbon contents (**Baker et al., 2002**). Careful chemistry control during steelmaking is therefore crucial to ensure suitable amounts of carbon remain in solution in the final product.

During slow cooling of batch annealed EDD grade steels almost complete precipitation of the carbon occurs and thus the remaining solute carbon is insufficient to cause bake hardening. To obtain bake hardening effect in batch annealed EDD, very low carbon grades of C~ 0.01% with some elements, like phosphorous, that increase carbon concentration in solution are employed. (**Beranger et al.)**.

While in the case of continuous annealing, the carbon level in solid solution at the end of annealing is quite high and the solute carbon can produce strengthening (70-80 MPa) by bake hardening (steel book). Care must be taken, however, with overaging practice during annealing, to ensure an appropriate amount of carbon (15-25 ppm) is left in solution in the final product.

7.3 Bake hardening IF steels

IF steels contain very low amounts of total carbon (~0.004%) (**Baker et al., 2002**).. In these steels all the interstitial elements are removed from solution by addition of carbide and nitride formers such as aluminium, titanium, niobium. These steels do not exhibit bake hardening as they have no interstitial elements in solution. However, the chemistry and

processing of these steels, can be adjusted to leave 15 -25 ppm carbon in solution, to render bake hardening effect for increasing strength by 30 - 60 MPa . There are several types of IF steels and in the following sections Ti-only, Nb-only and Ti+Nb steels will be discussed for bake hardening.

7.3.1 Titanium stabilized interstitial free bake hardening steels

This mechanism of precipitation applies only when some titanium remains in solution: in just stabilized or understabilized chemistries, formation of TiC and $Ti_4C_2S_2$ is inhibited because of the low titanium content (Baker et al., 2002). This successive precipitation of carbides and carbosulphides makes it difficult to control the amount of titanium available for carbon stabilization and thus the solute carbon content. However, a bake hardening product can be produced from a titanium chemistry by inhibiting or avoiding TiC formation, so that the total carbon content remains in solution and is available for bake hardening.

Work by Tanioku et al. (**Tanioku et al., 1991**) and Kojima et al. (**Kojima et al., 1993)** showed that this can be achieved by controlling total carbon at 15 -25 ppm and titanium at ~ 0.01%. The manganese content must be kept low (~ 0.3%) to prevent the formation of MnS in preference to TiS and the slab reheat temperature must be high (~ 1200°C) to prevent the precipitation of $Ti_4C_2S_2$. Another method for producing titanium IF bake hardening steels, discussed by Tsunoyama et al. (**Tsunoyama et al, 1998**) relied on reducing the sulphur level to minimize formation of TiS, as the role of TiS as a heterogeneous nucleation site for the precipitation of TiC can lead to the reduction in solute carbon and hence bake hardening response. Kawasaki et al. (**Kawasaki et al., 1991**) used a philosophy, involving a reduced sulphur level (0.005%) in association with an increase in manganese to 1.0% and thus, the formation of $Ti_4C_2S_2$ was suppressed, leaving carbon in solution and producing a bake hardening steel.

7.3.2 Niobium stabilized interstitial free bake hardening steels

Niobium is a strong carbide former that can stabilize carbon as NbC when added according to the stoichiometric ratio:(%Nb)=7.75(%C) (**Baker et al., 2002**).).

Nitrogen is stabilized by the addition of aluminium to form AlN. This is more stable and thus forms at higher temperatures than Nb(C,N), so it can be assumed that all niobium is available for carbide formation. The relative simplicity of carbon stabilization in these steels makes them ideal for the production of bake hardening grades. Control of solute carbon in the niobium bearing bake hardening steels can be achieved in two ways. First, insufficient niobium can be added fully to stabilize the carbon, leaving 15 - 25 ppm in solution after steelmaking. This methodology requires tight chemistry control during steelmaking and, because of the presence of solute carbon throughout subsequent processing, the rm-value can suffer.

The second method requires the full stabilization of carbon during steelmaking. Solute carbon is then liberated by solution of NbC during annealing. By annealing at high temperatures (800-850°C) and cooling at 420 Ks^{-1}, 15 -25 ppm carbon can be retained in solution (**Irie et al., 1982**). Since the carbon is fully stabilized until the end of annealing, r_m-

values in steels of this type are comparable with those of traditional IF grades. High temperature annealing of this kind can, however, lead to shape problems in the strip such as heat buckling. Some continuous annealing lines can operate at these high temperatures, but they are beyond the limits of conventional hot dip galvanizing lines. Steelmakers must therefore assess their own production capabilities before deciding on a suitable processing route for the niobium IF based bake hardening steels.

By reducing the sulphur level and increasing manganese, the formation of TiS can be suppressed, leaving all titanium available for nitrogen stabilization. The precipitation of $Ti_4C_2S_2$ can also be suppressed in this way, so carbon is controlled by niobium alone. As with the Nb only compositions, carbon content can be controlled either by understoichiometric addition of niobium, or by high temperature annealing and controlled cooling, depending on the capabilities of individual steelmakers. These steels have been widely researched and are the choice of many manufacturers.

7.3.3 Titanium and niobium stabilized interstitial free bake hardening steels

By reducing the sulphur level and increasing manganese, the formation of TiS can be suppressed, leaving all titanium available for nitrogen stabilization (**Baker et al., 2002**).). The precipitation of $Ti_4C_2S_2$ can also be suppressed in this way, so carbon is controlled by niobium alone. As with the Nb only compositions, carbon content can be controlled either by understoichiometric addition of niobium, or by high temperature annealing and controlled cooling, depending on the capabilities of individual steelmakers. These steels have been widely researched and are the choice of many manufacturers.

8. Recrystallization texture and drawability of bake hardening steels

Kitamura et al. (**Kitamura et al., 1994)** had presented a completely different methodology for the production of titanium based interstitial free bake hardening steels. The theory suggests that as the steel sheet absorbs carbon by annealing in a carburizing atmosphere, the Ti/C ratio decreases, eventually resulting in some solute carbon in the matrix. A bake hardening response of 20 -50 MPa was achieved in this way without compromising r value (**Figure 31**) (**Kitamura et al., 1994)**. Through this process, the reduction in r-value due to solute carbon in solution for interstitial free bake hardening steels can be eliminated as the steel remains fully stabilized by titanium and the excess carbon is introduced by carburizing atmosphere during annealing.

Xiaojun and Xianjin (**Xiaojun & Xianjin, 1995**) developed a new technology (the details were not mentioned) to improve the drawability of Ti+ Nb stabilized interstitial free high strength bake hardened steel. The r_m-value of the experimental sheet treated by the new technology is as high as 2.67, and this is the highest r_m-value published so far for phosphorus-added high strength and deep drawing sheet steels with increased strength due to bake hardening. Compared to conventional technology **(Figure 32a),** the new technology annealing rolling texture **(Figure 32b)** exhibited strong {111} components and weak {100}. The crystal orientations corresponding to the peak values of orientation concentrations of the texture were found to be changed from conventional (111)(112) orientations to (111)(011) orientations for the new technology (Figure 33).
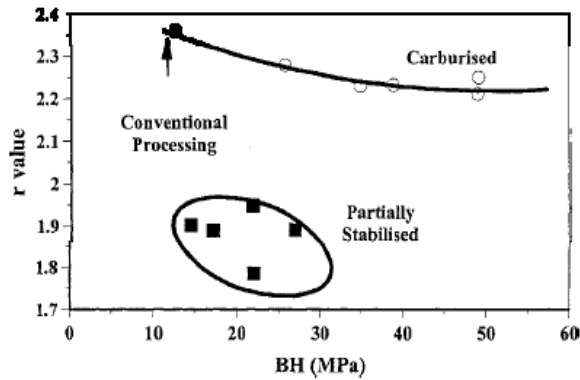
Fig. 31. Effect of processing on relationship between bake hardenability and r value for Ti-stabilized IF steel (**Kitamura et al., 1994**).
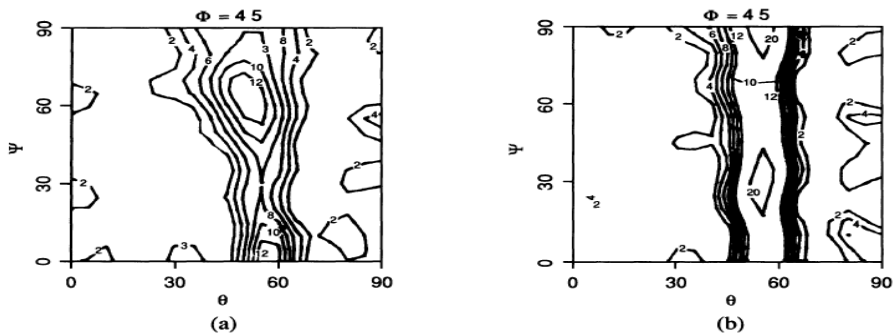

Fig. 32. φ=45° sections of ODFs of annealing textures obtained by two technologies respectively: (a) conventional processing and (b) new processing (**Xiaojun & Xianjin, 1995**).
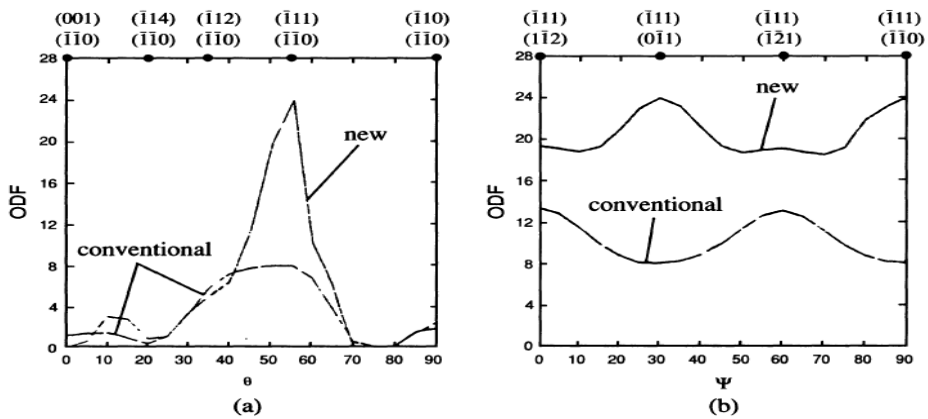

Fig. 33. Comparison of annealing textures obtained by two technologies respectively. (a) α-fiber axis textures (b) γ-fiber axis textures (**Xiaojun & Xianjin, 1995**).

Bake hardenability and drawability of IF steels with under- to over-stoichiometric atomic ratios of Ti/N and Nb/C were studied by Storojeva et al (http://www.cbmm.com.br/portug/sources/techlib/report/novos/pdfs/stabiliza.pdf). They observed that the r_m-value increased with a larger ferrite grain **(http://www.cbmm.com.br/portug/sources/techlib/report/novos/pdfs/stabiliza.pdf)** thus a high annealing temperature is favorable for good cold formability. The authors also reported that the r_m-value of the steels were higher that had lower solute carbon in the hot bands (**Storojeva et al., 2000**). This is confirmed (**Figure 34**) by just comparing the Ti+Nb containing steels, where the r_m-values of the steels with the high solute carbon in hot strip (12-14 ppm) were remarkably lower than those of the steels without any solute carbon in hot strip. However, the r_m-value of Ti-free, just Nb-containing steel with the high solute carbon content (14 ppm) in the hot strip was almost as high as in the Ti+Nb steels without any solute carbon. Thus, titanium free IF steel exhibits a lower recrystallization start temperature and by this means enhances r_m-value in the final product, allowing compensation of the negative effect of solute carbon in the hot band. **Figure 35** (**http://www.cbmm.com.br/ portug/sources/techlib/report/novos/pdfs/stabiliza.pdf)** summarizes test results of the r_m-value and BH-effect for annealing temperatures up to 840°C. It indicates, that a BH-effect >30 MPa together with r >1.7 can be obtained with the Ti-free, just Nb containing steel.
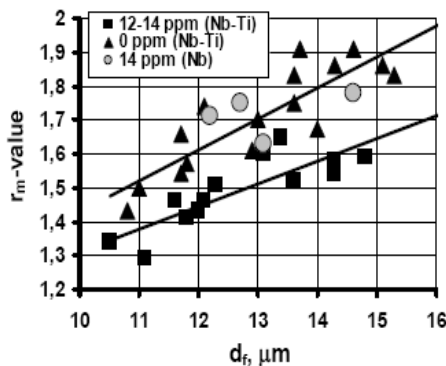

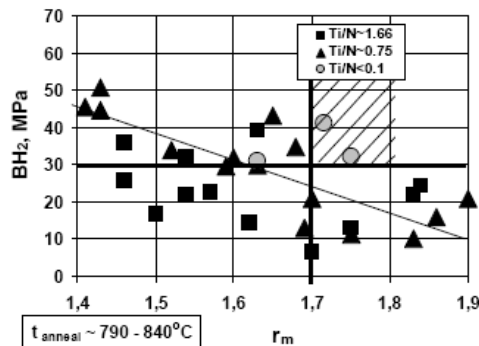Fig. 34. r_m- value of steels with various solute carbon in hot band of IF steels.

Fig. 35. r_m-value – BH-effect for Ti containing IF steels.

9. Recrystallization texture and drawability of warm rolled steels

The demand for thin and ultra thin rolled products led to an intensive search for alternatives to conventional hot and cold rolling processes. A number of studies were undertaken to investigate the advantages of rolling at temperatures between 850 and 500°C that is known as warm rolling (**Harlet et al., 1993**). Because of the lower reheat temperatures, warm rolling leads to lower production costs than hot rolling and requires significantly lower loads than cold rolling (**Harlet et al., 1993**). The latter factor means that higher reductions per pass can be produced by warm rolling than by cold rolling due to the lower plasticity of steel at room temperature. In conventional hot rolling, the finish rolling temperature is above the Ar3 temperature and in warm rolling finish rolling is made in the ferrite phase.

In the past years many researchers have worked on low, ultra carbon steels (**Sakata et al., 1997)** using warm rolling. The products obtained by ferritic hot rolling can be divided into two kinds according to the coiling temperature (**Mao, 2004).** One is a thin gauge soft and ductile hot rolled strip obtained by high temperature coiling for direct application that could be considered as a substitute for the conventional cold rolled and annealed sheet, and the other is a strained thin gauge hot strip gained by low temperature coiling for cold rolling and annealing, during which recrystallization texture strengthens by accumulating strains from hot rolling and cold rolling reductions.

Sa´nchez-Araiza et al (**Sa´nchez-Araiza, 2006**) reported on the texture changes in low carbon steel during recrystallization   and established the nucleation and growth mechanisms applicable to warm-rolled quantitatively.

The requirement necessary for the development of (111) texture is the accumulation of strain in the matrix and to achieve uniform accumulation of strain through the thickness of sheet steel, lubricant is required in addition to the optimization of Ti and Nb concentration **(Figure 36) (Sakata et al., 1997).** In 1996, Kawasaki Steel Corporation constructed a new hot strip mill in the Chiba works, where sheet bars are welded between the coil box and the finish mill to accomplish fully continuous rolling. This 'endless hot strip mill' makes lubricant rolling practical. The r_m-value achieved using warm rolling technique is 2.9. This value is noteworthy since the best value obtained in the conventional process does not exceed 2.6.

Wang et al (**Wang et al., 2007**) studied drawability of Ti-stabilized IF steel by finish rolling the steel at 760ºC in the ferritic region with lubrication and coiling at 740 and 400ºC. The evolution of texture for both the high and low temperature coiling is shown in in **Figures 37-40.** The optical micrographs of the test steels in hot rolled and high temperature coiled status, cold rolled as well as annealed one are shown in **Figure 37**. It can be seen from **Figure 37(a)** that after high temperature coiling, the deformed microstructure vanished and the recrystallization microstructure is characterized by uniform and equiaxed grains. **Figure 37(b)** shows that after cold rolling, the grains can not be discerned and the obvious characteristics of the cold rolled microstructure is the formation of the in-grain bands denoted by the arrow. As shown in **Figure 37(c),** deformed microstructure disappears and there are small and elongated grains after annealing. In order to obtain more equiaxed grains, the annealing temperature or the annealing time should be increased.
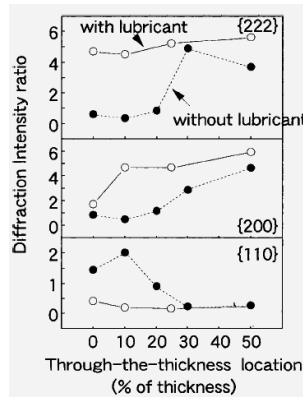
Fig. 36. Effect of lubricant on texture distribution through the thickness in ferrite rolled sheet steel; with finish rolling temperature 700 ºC, cold reduction 50%, and annealing time 20s at 850° C (**Sakata 16 et al., 1997**)
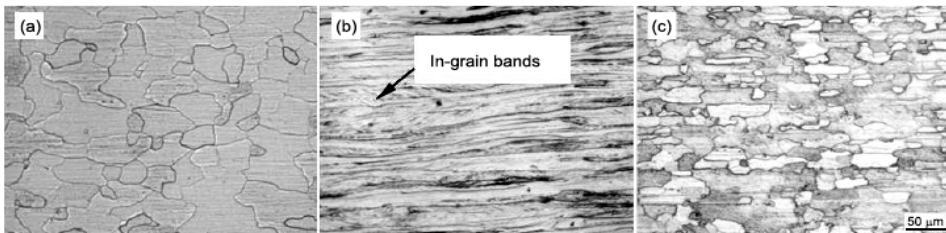

Fig. 37. Optical microstructures of samples in the condition of high temperature coiling: (a) hot rolled (b) cold rolled and (c) annealed samples (**Wang et al., 2007**).

Figure 38 shows the φ=45° ODF sections for high temperature coiled hot band, cold rolled and annealed sample. It is clear that after ferritic rolling and high temperature coiling, the most prominent texture intensity is along the γ-fiber and the maximum is at {111}<112>. Moreover, its characteristics are the same as that of the annealed texture in the condition of low temperature coiling, indicating that the hot band after high temperature coiling can be considered as a substitute for the conventional cold rolled and annealed sheet (**Wang et al., 2007).**
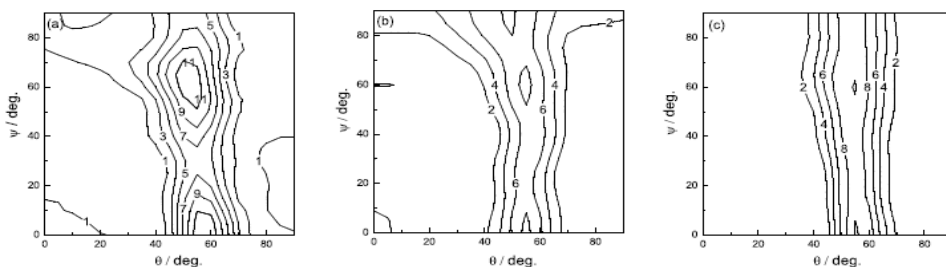

Fig. 38. φ=45º ODF sections in the condition of high temperature coiling: (a) hot rolled, (b) cold rolled and (c) annealed samples (**Wang et al., 2007**).

The optical micrographs of the low temperature coiled hot band, cold rolled as well as annealed one are shown in **Figure 39**. It is evident that a completely deformed microstructure is produced after hot rolling and low temperature coiling. Straighter grain boundaries and thinner deformation bands form after cold rolling. After annealing, the ferrite grains recrystallize completely, and small and uniform grains develop. **Figure 40** shows $\phi2=45^o$ODFs of low temperature coiled hot band, cold rolled and annealed samples. The texture of hot band includes a strong α-fiber whose peak is at {001}<110> as well as a weak γ-fiber whose main component is {111} <110>. The components in the α-fiber intensify and the intensity of {111}<112> in the α fiber changes little after cold rolling. A complete γ-fiber with the peak at {111}<112> develops and the components in γ-fiber weaken evidently after annealing.
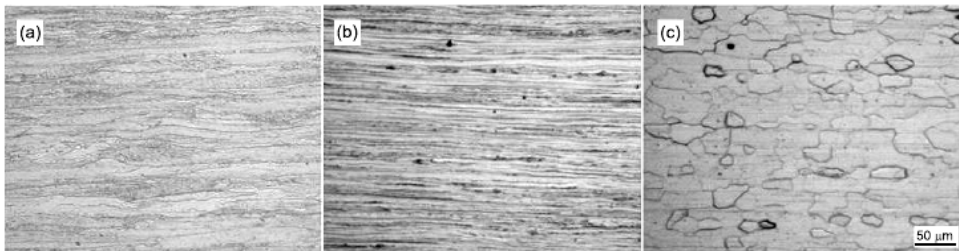

Fig. 39. Optical microstructures of samples in the condition of low temperature coiling: (a) hot rolled (b) cold rolled and (c) annealed samples (**Wang et al., 2007**).
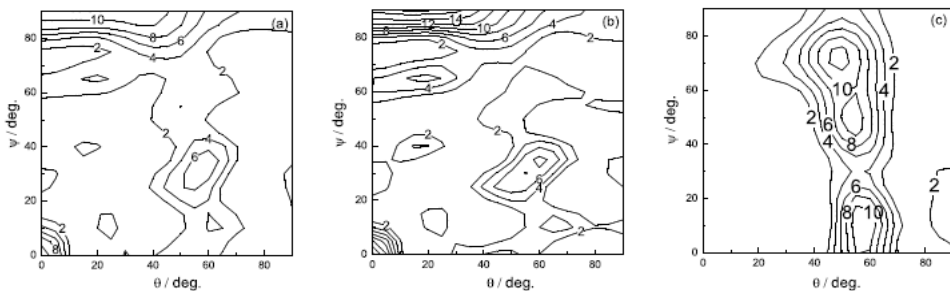

Fig. 40. $\phi=45^o$ ODF sections in the condition of low temperature coiling: (a) hot rolled, (b) cold rolled and (c) annealed samples (**Wang et al., 2007**).

In a study on the effect of chemical composition and ferritic hot rolling on the formation of texture in the hot rolled and coiled, cold rolled, and cold rolled and annealed Ti and Ti+Nb added IF steels, it was reported that high r_m-values could be obtained at the same intensity levels of {111}<110> texture component if the grain growth was inhibited by a suitable addition of microalloying elements. (**Tiitto et al., 2004**). While as per the conventional wisdom it is known that grain growth during annealing is beneficial for drawability as it increases the volume fraction of grains with the {111} texture, leading to higher r_m-value. It was claimed that due to the grain refining effect of Nb, a small addition of the element (100 ppm) to the Ti alloyed IF steel increased the r_m-values in the annealed condition by about 15% at the same {111}<110> intensity levels. Thus, ferritic hot rolling seemed to be beneficial only if it contributed to the development of a strong intensity of the γ -fiber texture in

association with a uniform and small grain size during annealing. Further they added, hot deformation of Nb and Ti alloyed steels at a high temperature (870°C) in the ferritic region led to higher {111}<110> intensities and higher r- values in the annealed condition than hot deformation at a lower temperature (800°C).

The development of the γ-fibre in annealed steels was linked (**Barnett & Jonas, 1997a; Duggan et al., 2000**) to the presence of a high volume fraction of grains containing shear bands after warm rolling. These bands appear to be the nucleation sites for recrystallised grains of the desirable orientation. After warm rolling, many of the grains in interstitial-free (IF) steels contain such shear bands and the steels then exhibit good forming characteristics after annealing (**Barnett, 1998**). By contrast, in low carbon steels, the presence of carbon in solid solution leads to dynamic strain aging during warm rolling and to high positive rate sensitivities. The latter prevent the formation of high densities of in-grain shear bands, leading to a lack of nucleation sites for the γ-fibre during annealing.

Timokhina et al (**Timokhina et al., 2004**) studied the effect of in grain shear bands on the volume fraction of favourable γ-fibre in IF, low carbon (LC) and LC with Cr, P and B added steels. Shear bands are usually contained within single deformed grains and are tilted by 20–35° with respect to the rolling plane. There are four types of in-grain shear bands: long (5-40 µm long--±15-40o to rolling direction), short (0.5-15 µm long), intense short (0.4-7 µm, ±5-45o) and intense long (continuous wavy lines--±15-40o to rolling direction) (**Barnett & Jonas, 1997b**) as shown in **Figure 41.** All the grains containing shear bands were characterized by zones of grain boundary displacement or stepping that provide evidence for local flow along the bands (**Barnett, 1996**). The presence of moderate amounts of long shear bands in IF steels was attributed to the formation of the γ-fibre after annealing (**Barnett & Jonas, 1997a**).
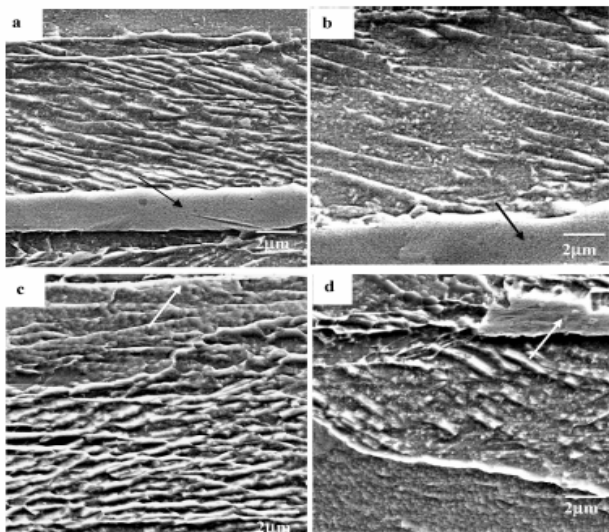

Fig. 41. SEM micrographs of (a) long shear bands (b) short shear bands, (c) intense long shear bands and (d) intense short shear bands. Arrows indicate the displacement zones (**Barnett & Jonas, 1997b**).

In their study, Timokhina et al (**Timokhina et al., 2004**) reheated the sample to 1050ºC for 30 mins and subsequently warm rolled by 65% in a single pass pilot mill. Temperatures of 640ºC and 710ºC and average strain rates of 30s^{-1} were employed followed by quenching. To establish grain orientation with different sheer bands, the grains were marked with hardness tester prior to electron back scattered diffraction analysis. The addition of alloying elements was observed to affect different types of shear band and the formation of γ -fibre. The IF steel was characterized by the largest number of grains with long shear bands with γ -fibre, 65 % and 67 % in the steels rolled at 640°C and 710°C respectively. Increasing the amount of carbon and decreasing the grain size, as in the LC steel, increased the proportion of grains with the short shear bands. Further, the proportion of grains containing intense long shear bands was higher in the LC steel than in the IF grade. The addition of carbon perceptibly decreased the volume fraction of grains with γ-fibre. The addition of chromium led to the formation of similar volume fractions of grains with short, long and intense long shear bands at both rolling temperatures. This led to an increase in the number of grains with beneficial γ -fibre to 46–47% compared to 25–26 % in the LC steel. However, in a subsequent study Pereloma et al (**Pereloma et al., 2004**) reported that although the formation of chromium carbides in the microstructures of the LC-Cr and LC-Cr+P steels removed carbon from solid solution and in this way slightly increased the fraction of γ-fiber nuclei formed at shear bands, the effect led to a reinforcement of the ND component (γ-fiber) only in the early stages of recrystallisation. The strength of γ-fiber gradually deteriorated with the progress of recrystallisation. The reasons put forward for this undesirable development were i) the retarding effect of the carbides on the mobility of grain boundaries during growth, ii) the influence of the particles on nucleus rotation during annealing and iii) the absorption of γ-fiber nuclei by other components during grain coalescence and growth. Thus, further study of the texture behaviour during grain coalescence and growth was required.

The addition of boron suppressed the formation of long, short and intense long shear bands and assisted in the formation of intense short shear bands that, in turn, decreased the volume fraction of grains with γ -fibre. The addition of phosphorus, on the other hand, increased the long and short shear band frequency and the proportion of grains with γ -fibre. In the Cr–B–Ti modified steel, the short, long and intense long shear bands were absent and they were replaced by intense short shear bands.

Jing et al (**Jing et al., 2011**) analyzed the grain boundary and microtexture characters of a rephosphorised high strength IF-steels under 700 and 800ºC warm-rolled temperatures to observe the effect on deep drawability. It was found that while the samples were rolled at 700°C, more γ-fiber texture components, {111}<112>, {111}<110>, {554}<225>, low angle and CSL grain boundaries were formed that were beneficial for deep-drawability. However, the samples that were rolled at 800°C, manifested more α-fiber texture components and high angle grain boundaries that led to inferior deep drawing property. The average r-value was 1.32 for the samples rolled at 700°C and 1.05 for those that were rolled at 800°C, respectively.

Recrystallization texture investigation for IF-Ti and Ti stabilized IF-HS was conducted by Wang et al (**Wang et al., 2006**) under ferritic hot rolling and high-temperature coiling. Comparing with the completely recrystallized textures of the ordinary IF steel, the textures of the high-strength IF steel were of deformation type. This was attributed to the high phosphorous content in the high-strength IF steel that prevented recrystallization during the coiling process. For the ordinary IF steel, the texture components were mainly very weak

rotated cube component {001}<110>at the surface, and partial α-fiber with key orientation {223}<110>orientation and <111>||ND texture at the mid-section and 1/4-section. While, for the high-strength IF steel, the texture components were orientation (Goss) at the surface and a sharp α-fiber extending from {001}<110> to {223}<110⟩ in association with a Weak <111>||ND texture at the mid-section and 1/4-section.

In another work by Ferry et al. (**Ferry et al., 2001**) on ultra low carbon steel (0.0036C, 0.03Ni, 0.019Mn, 0.03Al, 0.004Ti and 0.003N) it was found that the hot deformation microstructure had a strong influence both on the kinetics of recrystallization and texture development during cold rolling and annealing. In particular, a warm-deformed ferrite microstructure (lower finish deformation temperature (FDT)) recrystallized most rapidly to produce a strong <111>||ND recrystallization texture (γ -fibre) as it produces as-strained α in combination with the additional strain by cold rolling, which result in rapid recrystallization. while an initial coarse-grained ferrite microstructure recrystallized most sluggishly to produce a strong {001}<110> texture due to copious nucleation of grains at shear bands, which is consistent with previous studies (**Hutchinson, 1984; Muljono, 2001**). **Figure 42** (**Ferry et al., 2001**) shows φ$_2$=45° ODF sections in the fully recrystallized cold rolled and annealed samples following hot deformation at three significant finish rolling temperatures: (a) 920°C (fine, equiaxed ferrite), (b) 850°C (coarse ferrite) and (c) 600°C (warm deformed ferrite). The maximum intensity of the two most dominant recrystallization texture components, {001}<110> and {111}//ND, as a function of FDT are given in **Figure 43** (**Ferry et al., 2001**). It can be seen that the development of the strongest {111}//ND CRA texture is favoured when FDT is: (i) greater than 870°C (which produces fine-grained ferrite by transformation), and (ii) below, 800°C (which also produces fine-grained ferrite but with an additional true strain of 0.8 prior to cold rolling). Thus, it is indicated that warm rolling has a significant influence on final texture after cold rolling and annealing and warm rolling is capable of strengthening the {111}//ND (γ-fiber) recrystallization texture that is the favourable texture for drawability in the production of formable ultra low carbon steel sheets.
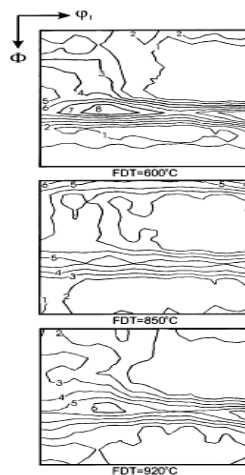

Fig. 42. φ$_2$=45° sections in Euler space showing recrystallization textures of the ultra low carbon steel with FDTs 600°C, 850°C and 920°C (contours: 1, 2, 3...random) (**Ferry et al., 2001**).
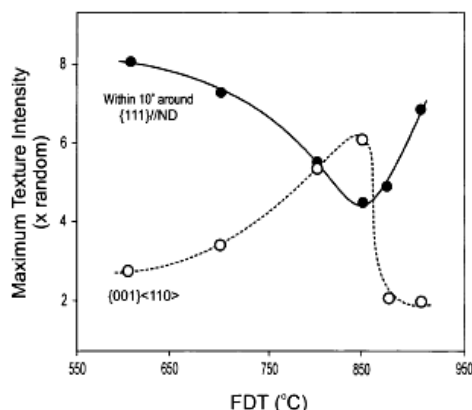
Fig. 43. Effect of FDT on maximum texture intensity of {001}<110> and within 10° around <11l>||ND (γ -fibre) of the annealed ultra low carbon steel (the maximum intensity is taken from the each calculated ODF) (**Ferry et al., 2001**).

10. References

Auburn, Ph. & Rocquet P. (1973). Mem. Sci. Rev. Met., Vol. LXX, No. 4, p. 261.

Baker L. J., Daniel S. R & ParkerJ. D. (2002). Mater. Sci. Technol. Vol. 18, No. April, pp. 355-367.

Banerjee K., Verma A. K. & Venugopalan T.(2008). Metall. and Mater. Trans. A, Vol. 39, No. June, pp. 1410-1425.

Barnett M. R. & Jonas J. J. (1997). ISIJ Int., Vol. 37 pp. 697-705.

Barnett M. R. & Jonas J. J. (1997). ISIJ Int., Vol. 37, pp. 706-714.

Barnett M. R. & Jonas J. J. (1999).ISIJ Int., Vol. 39 pp. 856-873.

Barnett M. R. (1996).Ph.D. Thesis, McGill University, p. 52.

Barnett M. R. (1998). ISIJ Int., Vol. 38 pp. 78-85.

Barnett M.R. & Kestens L.(1999). ISIJ Int., Vol. 39, pp. 923-929.

Barrett M.R. & Jonas J.J.(1997) , ISIJ Int., Vol. 37, pp. 706-714.

Beranger G., Henry G & Sanz G. 1996.The book of Steel, Springer-Verlag, USA, 2-85206-981-18 (1994), USA, pp. 935-951.

Cao W. D. , Lu X. P. , Sprecher A. F. & Conrad H. (1990). Mater. Lett., Vol. 9, p. 193.

Cao S. Q. (2005). Grain Boundaries and the Evolution of Texture in Interstitial-free (IF) Steels, Ph.D. Thesis, Shanghai Jiao Tong University.

Chung J. , Era H. & Shimizu M. (1987). Metall. Trans. A, Vol. 18, No. June , pp. 957-968.

Conrad H. , Guo Z. , Sprecher A. F. (1989). Scripta Metall .Vol. 23, pp. 821-823.

Doherty R.D. (1985). Scr. Metall., Vol. 19, pp. 927-930.

Doherty R.D. , Hughes D.A. , Humphreys F.J. , Jonas J.J., Juul Jensen D., Kassner M.E., King W.E., McNelley T.R. McQueen H.J. & Rollett A. D. (1997). Mater. Sci. Eng. A, Vol. 238, pp. 219–274.

Duggan B. J. , Liu G. I. , Ning H. , Tse Y. Y. (2000). Proc. Int. Conf. Thermomechanical Processing of Steels, IOM Communications Ltd. London, UK, pp. 365 - 371.

El-Kashif E., Asakura K. & Shibata K. (2003). ISIJ Int., Vol. 43, No. 12, pp. 2007-2014.

Ferry M., Yu D. & Chandra T. (2001). ISIJ Int., Vol. 41, No. 8, pp. 876–882.

Gupta I. and Bhattacharya D. (1990). Metallurgy Of Vacuum Degassed Steel Products, ed. R. Pradhan, TMS, Warrendale, PA, TMS, pp 43– 72.

Harlet P. , Beco F. , Cantinieaux P. , Bouquegneau D. , Messien P. & Herman J. C. (1993). Int. Symp. on Low C Steels for the 90's, eds. R. Asfahani & G. Tither, TMS-AIME, Warrendale, PA, p. 389.

Hatherly M. & Hutchinson W. B. (1979). An introduction to textures in metals, The Institution of Metallurgists, Monograph 5.

He C.S. , Zhang Y.D., Wang Y.N. , Zhao X. , Zuo L. & Esling C. (2003). Scripta Mater., Vol. 48, pp. 737–74.

Hebert V., Louis P. , Zimmer P. & Delaneau P. (1992), CESSID document 92154.

Heckler A. J. & Granzow W. G. (1970). Metall. Trans A, Vol. 1, pp. 2089-94.

Held J. F. (1965). Mechanical Working and Steel Processing IV, ed.D. A. Edgecombe, American Institute of Mining, Metallurgical and Petroleum Engineers, New York, p. 3.

Holie S. (2000). Mater. Sci .Technol., Vol 16, pp. 1079-1093.

Hölscher M. , Raabe D. & Lu¨cke K. (1991). Steel Res., Vol. 62, No. 12, pp. 567-75.

Hook R. E. (1990). Metallurgy of vacuum-degassed steel products (ed. R. Pradhan), 1990, Warrendale, PA, Metallurgical Society AIME, p.263.

Hosford W. F. & Backholen W.A. (1964). Fundamentals of deformation processing, Syracuse, Press, New York. P. 259.

Hu H. & Goodman S.R. (1970). Metall. Trans., Vol. 1, pp. 3057-64.

Hu H. (1977). Metall. Trans. A, Vol. 8, pp. 1567-75.

Hughes I.F. & Page E.W. (1971). Metall. Trans., Vol. 2, pp. 2067-75.

Hutchinson W. B. (1984). Intl. Mater. Reviews, Vol. 29, No. 1, pp. 25-42.

Hutchinson W.B. & Ushioda K. (1984). Scand. J. Met., Vol. 13, p. 269-284.

Irie T. , Hashiguchi H. , Satoh S. , Konoshi M. , Takahashi K. & Hashimoto M (1981).Trans. Iron Steel Inst. Jpn., Vol. 21, No. 11, pp. 793-801.

Irie T. , Satoh S. , Yasuda A. & Hashimoto O. (1982). Metallurgy of Continuously Annealed Sheet Steel, TMS, Warrendale, PA, TMS, pp. 155-171.

Jeong W. C. (2000). Metall. and Mater. Trans. A, Vol. 31, No. April, pp. 1305-1307.

Jing C. , Wang M. , Liu X. , Tan Q. , Wang Z. & Han F. (2011). Mater. Sci. Forum, Vol. 682, pp. 71-74.

Juntunen P. , Raabe D., Karjalainen P. , Kopio T. & Bolle G. (2001). Metall. & Mater. Trans. A, Vol. 32, No. Aug, pp. 1989-95.

Kang H. , Garcia C. I. , Chin K. & DeArdo A. J. (2007). ISIJ Int., Vol. 47 No. 3, pp. 486–492.

Katoh H. , Takechi H. , Takahashi N. & Abe M. (1985). Int. Conf. on Technology of Continuously Annealed Cold Rolled Sheet Steels, ed. Pradhan. R, Proc. . TMS-AIME, Warrendale, PA, USA, pp. 37-60.

Kawasaki K., Senuma T. & Sanagi S. (1991). Processing, Microstructure and Properties of Microalloyed and other Modern HSLA Steels, ISS, Warrendale, PA, pp. 137 - 144.

Kestens L.., Jonas J. J., Van Houtte P. & Aernoudt E. (1996). Textures and Microstructures, Vol. 26-27, pp. 321-335.

Kim S., Choi I., Park I. & K. Cho (2005). Mater. Sci. Forum, Vol. 475-479, pp. 475-479.

Kitamura M. , Tsukatani I. & Inoue T.(1994) : ISIJ Int., Vol. 34, No. 1, pp. 115 – 122.

Klein A. J. & Hitchler, E. W. (1973). Met. Eng. Q., Vol. 13, pp. 25—27.

Kojima N. , Mizui N.& Tanioku T. (1993). Sumitomo Search, Vol. 45, No. 5, pp.12 – 19.

Kozeschnik E. , Pletenev V. , Zolotorevsky N. & Buchmayr B. (1999) , Metall. & Mater Trans. A, Vol. 30, No. June, pp. 1663-1673.

Krauss G., Wilshynsky D. O. & Matlock D. K. (1991). Interstitial Free Steel Sheet: Processing, Fabrication and Properties, eds. L. E. Collins and D. L. Baragar, CIM/ICM1, Ottawa, pp. 1- 14.

Lankford W. T. , Snyder S. C. & Bauscher J. A. (1950). Trans.AS1/I, Vol. 42, pp.1197 — 1232.

Lebrun J. L., Maeder G. & Parniere P.(1981) : Proc. 6th Intl. Conf on Texture of Materials, Vol. 2, Tokyo, The Iron and Steel Institute of Japan, p. 787.

Mao X. (2004). Iron Steel, Vol. 39, No. 5, p. 71.

Martin, J.W., Doherty R. D. , Cantor B. (1997). Stability of Microstructure in Metallic Systems (2nd edition)., Cambridge University Press, Cambridge.

Matlock D. K., Allan B. J. & Speer J. G. (1998). Proc. Conf. Modern LC and ULC Sheet Steels for Cold Forming Processing and Properties, ed. W. Bleck, Aachen, Verlag Mainz, pp. 265 - 276.

Matsudo K. , Osawa K. & Kutihara K. (1984). Technology of Continuously Annealed Cold-Rolled Sheet Steel, ed. R. Pradhan, TMS-AIME, Michigan, pp. 3-36.

McQueen H.J. , Rollett A.D. (1997). Materials Science and Engineering, Vol.A238, pp. 219–274.

Mendoza R. , Huante J. , Alanis M., Gonzalez-Rivera C. & Juarez-Islas J. A. (2000). Mater. Sci. Eng A, Vol. 276, pp. 203-209.

Mendoza R. ,Alanis M. , Aramburo G. , Serrania F. & Juárez-Islas J.A. (2004). Mater. Sci. Eng.A, Vol. 368, pp. 249–254.

Meyzaud Y.& Parniere P.(1974). Mem. Sci. Rev. Met., Vol. LXXI, No. 7-8, pp. 423.

Mizui N. , Okamoto A. & Tanioku T.(1990). Proc. LTV/SMI Technology Exchange Meeting, Ltv Steel/Sumitomo Metal Industries.

Muljono D. , Ferry M. & Dunne D.P.(2001). Mater. Sci. Eng. A, Vol. 303, pp. 90–99.

Nishimoto A. , Inagaki J. & Nakaoka K.(1982).Tetsu-to-Hagne, Vol. 68, pp.1404-1410.

Ono S. , Shimomura T., Osawa K. & Matsudo K.(1982). Transaction ISIJ, Vol. 22, pp. 732-738.

Park Y.B. , Kestens L.& Jonas J.J. (2000). ISIJ Int., Vol. 40, pp. 393-401.

Pereloma E. V. , Timokhina I. B. , Nosenkov A. I. & Jonas J. J. (2004). Metallurgija, Vol. 43, No. 3, pp. 149-154.

Perera M., Saimoto S. & Boyd D. (1991). Interstitial Free Steel Sheet: Processing, Fabrication and Properties, eds.. L. E. Collins and D. L. Baragar, ;Ottawa, CIM/ICM, pp. 55 - 64.

Ray R. K. & Jonas J. J. (1990). Int., Mater. Rev., Vol. 35, No. 1, pp. 1-36.

Ray R. K., Jonas J. J. & R. E. Hook (1994). Intl. Mater. Reviews, Vol. 39, No. 4, pp. 129-172.

Rege J. S. , . Garcia C. I & DeArdo A. J.(1997). Proc. 39th Mechanical Working and Steel Processing, Vol. 35, ISS, Warrendale, PA, USA, pp. 149-158.

Rege J. S., Hua C., Garcia I. & DeArdo A. J. (2000). ISIJ Intl., Vol. 40, No. 2, pp.191-199.

Ruiz-Aparicio L.J. , Garcia C.I. & Deardo A.J. (2001) , Metall.and Mater. Trans. A, Vol. 32, No. September, pp. 2325-2334.

Sa´nchez-Araiza M. , Godet S. , Jacques P.J. & Jonas J.J. (2006). Acta Mater. , Vol. 54, pp. 3085–3093.

Sakata K. , Matsuoka S. , Obara T. , Tsunoyama K. & Shiraishi M.(1997). Materia. Japan, Vol. 36 No. 4 p. 376.

Samajdar I. (1994).Ph.D. Thesis, Drexel University.

Sarkar B., Jha B. K. & Deva A. (2004). J. Mater. Eng. and Perform., Vol. 13, No. 3, pp. 361-36

Schulz L. G. (1949). J. Appl. Phys. Vol. 20, No.11, pp.1030-33.

Song X., Yuan Z. Jia J. , Wang D. , Li P. & Deng Z (2010). J. Mater. Sci .Technol. Vol. 26, No. 9, pp.793-797.

Storojeva L. , Escher C. , Bode R. , K. Hulka & Yakubovsky O. (2000). IF Steels 2000, ISS, Warrendale, PA, p. 289.

http://www.cbmm.com.br/portug/sources/techlib/report/novos/pdfs/stabiliza.pdf

Takahashi M., Okamoto, A. (1974). Sumimoto Met., Vol. 27,pp. 40-49.

Tanioku T. , Hobah Y. , Okamoto A. & N. Mizui (1991). SAE Technical Paper 910293, Society of Automotive Engineers, Warrendale, PA, USA.

Tiitto K. M. , Jung C. , Wray P. , Garcia C. I. & DeArdo A. J. (2004). ISIJ Int., Vol. 44, No. 2, pp. 404–413.

Timokhina I. B. , Nosenkov A. I. , Humphreys A. O. , J. J. Jonas & Pereloma E. V.(2004). ISIJ Int., Vol. 44, No. 4, pp. 717–724.

Tither G. & Stuart H. (1995). HSLA Steels '95', ed. L. Guoxun et al.., Chinese Society for Metals, Beijing, pp. 22-31.

Tither G., Garcia C. I., Hua M. & Deardo A. J. (1994). Int. Forum for. Physical Metallurgy in IF Steels, Iron and Steel Institute of Japan, Tokyo, pp. 293-322.

Tokunaga Y. & Yamada M. (1985). Method for the Production of Cold Rolled Steel Sheet Having Super Deep Drawability, US Patent 4,504,326.

Tokunaga Y. & Kato H. (1990). Metallurgy of Vacuum Degassed Products , TMS, Warrendale, PA, pp. 91 -108.

Tsunoyama K. (1998). Phys. Stat. Sol. (A), Vol. 167, No. 427, pp. 427-433.

Tsunoyama K. , Sakata K., Obara T. , Satoh S. , Hashiguchi K. & Irie T.(1988). Hot and Cold Rolled Sheet Steels, eds. R. Pradhan and G. Ludkovsky, TMS, Warrendale, PA, pp. 155 - 165.

Tsunoyama K., Satoh S., Yamasaki Y. & Abe H. (1990). Metallurgy of Vacuum Degassed Products, 1990, TMS,   Warrendale, PA, pp. 127 -141.

Wang Y. N. , He C. S. , Zhao X. , Zuo L., Zhi Q. Z. & Liang Z. D (2000). Acta Metall Sinica, Vol. 36, No. 2, p. A126.

Wang Z. , Guo Y. , Xue W., Liu X. & Wang G.(2007). J. Mater. Sci. Technol., Vol. 23 No.3, pp. 337-341.

Wang Z.D. , Guo Y.H. , Sun D.Q. , Liu X. H. & Wang G.D. (2006). Mater. Charact., Vol. 57, No. 4-5, pp. 402-407.

Whiteley R. L. & Wise D. E (1962). Flat rolled products III, Interscience, New York, pp. 47─63.

Wilshynsky-Dresler D. O., Matlock D. K. & Krauss G. (1995): ISS Mech. Work. Steel Process. Conf., 1995, 33, pp. 927 – 940.

Wilson D. V. (1966). J. Inst. Met., Vol. 94, pp. 84─93.

Xiaojun G. & Xianjin W. (1995). Textures and Microstructures, Vol. 23, pp. 21-27.

Yasuhara E., Sakata K. , Furukimi O. & Mega T. (1996): Proc. 38th Mechanical Working and Steel Processing, Vol,. 34, Cleveland, Ohio, USA, pp. 409-415.

Yoshicla K. at. (1974): Deep Drawing Research Group, Proc. 8th Biennial IDDIG Congr. Gothenburg, 1974, pp. 258─268.
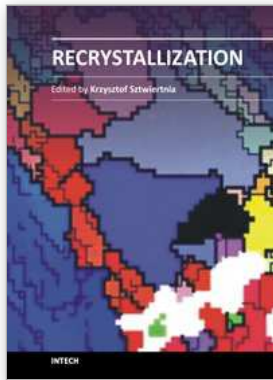
Recrystallization

Edited by Prof. Krzysztof Sztwiertnia

Recrystallization shows selected results obtained during the last few years by scientists who work on recrystallization-related issues. These scientists offer their knowledge from the perspective of a range of scientific disciplines, such as geology and metallurgy. The authors emphasize that the progress in this particular field of science is possible today thanks to the coordinated action of many research groups that work in materials science, chemistry, physics, geology, and other sciences. Thus, it is possible to perform a comprehensive analysis of the scientific problem. The analysis starts from the selection of appropriate techniques and methods of characterization. It is then combined with the development of new tools in diagnostics, and it ends with modeling of phenomena.

How to reference

In order to correctly reference this scholarly work, feel free to copy and paste the following:

Kumkum Banerjee (2012). Physical Metallurgy and Drawability of Extra Deep Drawing and Interstitial Free Steels, Recrystallization, Prof. Krzysztof Sztwiertnia (Ed.), ISBN: 978-953-51-0122-2, InTech, Available from: http://www.intechopen.com/books/recrystallization/physical-metallurgy-and-drawability-of-extra-deep-drawing-and-interstitial-free-steels

INTECH
open science | open minds